Optimal flow for general multi-carrier energy systems,including load flow equations

Markensteijn, A.S.; Romate, J.E.; Vuik, Cornelis

Important note
To cite this publication, please use the final published version (if applicable).
Please check the document version above.

DELFT UNIVERSITY OF TECHNOLOGY

REPORT 20-06

Optimal flow for general multi-carrier energy systems,
including load flow equations.

A.S. Markensteijn, J.E. Romate, C. Vuik

Optimal flow for general multi-carrier energy systems, including load flow equations.

A.S. Markensteijn, J.E. Romate, C. Vuik

December 16, 2020

Abstract

Optimization is an important tool for the operation of an energy system. Multi-carrier energy systems (MESs) have recently become more important. Load flow (LF) equations are used within optimization to determine if physical network limits are violated. The way these LF equations are included in the optimal flow (OF) problem, influences the solvability of the OF problem and the convergence of the optimization algorithms. This paper considers two ways to include the LF equations within the OF problem for general MESs.

In the first formulation, optimization is over the combined control and system-state variables, with the the LF equations included explicitly as equality constraints. In the second formulation, optimization is over the control variables only. The system-state variables are solved from the LF equations in a separate subsystem, given the control variables. Hence, the LF equations are included only implicitly in the second formulation. The two formulations are compared theoretically. The effect of the two formulations on the solvability of the OF problem is illustrated by optimizing two MESs.

Both formulation I and formulation II result in a solvable OF problem. For the two example MESs, the optimization algorithms require significantly fewer iterations with formulation II than with formulation I. For formulation II, the direct and the adjoint approach can be used to determine the required derivatives within the optimization algorithms. Scaling is needed to solve the OF problem for MESs. Both matrix scaling and per unit scaling can be used, but they are not equivalent.

Contents

1 Introduction

Multi-carrier energy systems (MESs) have become more important, as the need for sustainable energy systems increases. Single-carrier energy systems, such as power grids or gas networks, are coupled to form one integrated or multi-carrier energy system. Due to increased flexibility, reliability, use of renewables and distributed generation, and due to reduced carbon emission, MESs can give better performance than classical energy systems. An overview of MESs is given in [1].

Optimization is an important tool for the operation of an energy system. The distribution of generation over the various sources, or the set points of controllable elements, are determined such that some objective is optimized. At the same time, the operation of the energy system must stay within physical limits. Optimization for single-carrier systems, especially power grids, has been widely studied, but optimization for MESs has only been proposed recently. Load flow equations, or network equations, are used in finding an optimal solution and to determine if physical limits are violated. The way these load flow equations are included in the optimization problem influences the solvability of the optimization problem. Most optimization problems for MES simplify these equations, or do not consider network transmission at all.

In [2], social welfare is maximized for a combined gas and electricity network. The load flow equations are included as equality constraints. However, there is only a single point of coupling between the two networks, and the boundary conditions are chosen such that the load flow problem for electricity can be solved independently of that of gas. In [3], a general optimization framework for MESs is introduced. They use the energy hub (EH) concept, which is a linear model for the coupling units assuming uni-directional flow, which limits the generality. In [4], the total operation costs of an integrated gas, electricity, and heat network are minimized, also using EHs for the coupling models. In [5], the operation costs of a combined gas and electricity network are minimized, by decomposing the coupled problem in a gas problem and an electrical problem. In [6], an integrated gas, electricity, and heat network is optimized, where the thermal equations are decoupled from the other constraints, and a linear model for heat exchangers is used. In [7], an optimal dispatch problem is used, considering only energy balances instead of detailed load flow equations. In [8], an integrated gas, electricity, and heat network, including storage, is optimized. The optimization and network simulation are decoupled, such that a linear approximation of the network equations is used within the optimization.

Various formulations of the load flow equations exist for modeling energy systems, both in the single-carrier and in the multi-carrier case. Moreover, there are multiple ways to incorporate the load flow equations in the optimization problem. Usually, the load flow equations are directly included in the optimization problem as equality constraints. Nonlinearities of these constraints cause issues with convexity and solvability of the optimization problem, as also noted in [3] and [6]. Hence, the formulation of the load flow equations, and the way they are incorporated in the optimization problem, greatly influence the solvability of the optimization problem.

An important factor for practical solvability of optimization problems is scaling. Due to the various orders of magnitude of the physical quantities in energy systems, an unscaled optimization problem for MESs is generally badly scaled. Therefore, scaling greatly improves solvability of the optimization problem and convergence of the optimization algorithm.

To the best of the authors knowledge, the effect of the formulation of the load flow equations, of the way they are incorporated in the optimization problem, and the effect of the type of scaling on the solvability of optimization problem has not been studied.

In this work, we provide an analysis of the effect of the load flow equations on the solvability of the

optimization problem for general MESs. We formulate an optimization problem for a general single- or multi-carrier energy system, providing a general optimization framework. Total energy generation costs are minimized, where the optimal solution is required to satisfy the physical operational limits of the energy system. The load flow equations are included either explicitly as equality constraints or they are included implicitly as subsystem. In the latter, the steady-state load flow problem is solved as a subproblem of the optimization problem. We give a qualitative analysis of the resulting optimization problems by comparing, amongst others, nonlinearity, feasibility, problem size, and solvability. Furthermore, we consider the effect of scaling on the solvability of the optimization problem.

We show that the optimization problem of MESs is solvable when the load flow equations are included as equality constraints and when the are included as subsystem. This allows for various formulations of the load flow equations, within an optimization framework. Both ways of incorporating the load flow equations have advantages and disadvantages. The best way to formulate the optimization problem, and the load flow equations, depends on the MES and the specific problem at hand. Furthermore, we show that scaling is crucial for convergence of the optimizer.

In Section 2, the steady-state load flow problem of general MESs is stated. In Section 3 we formulate the optimization problem. First, we give the objective function to be minimized. Then, the effect of which network quantities are chosen as variables and which are considered known is discussed. We describe the two ways of including the load flow equations, that is as equality constraints or as subsystem, within an optimization framework. Based on this, two formulations of the general optimization problem for MESs are stated. Advantages and disadvantages of both formulations are discussed. In Section 4 we give the methods used for solving the optimization problem. Various optimizers suitable for the two optimization problems are used. We give two ways of scaling the optimization problem: per unit scaling and matrix scaling. Finally, two approaches for calculating the required (partial) derivatives of the objective function and constraints when the load flow equations are included as subsystem are introduced. The two formulations of the optimization problem, both with and without scaling, are used to optimize example MESs in Section 5, demonstrating some of the theoretical advantages and disadvantaged of the formulations of the optimization problem in practice.

2   Steady-state Load Flow

Steady-state simulation of an energy system, sometimes called steady-state load flow (LF), is the problem of determining the flows and other quantities of interest in the energy system, given constant demands. See for instance [9] for a single-carrier electrical system, [10] for a single-carrier gas system, and [11], [12], or [13] for MESs. We use a slightly adjusted model of the LF model described in [13] for MESs.

For the steady-state problem, the energy system is mathematically represented as a graph. The quantities of interest, and their relation to the graph representation, are shown in Figure 1 for a single-carrier gas, electricity, and heat network, and for a coupling node. In this graph representation, terminal links are used to model inflow and outflow of the energy network. Figures 1a–1c show single-carrier gas, electricity, and heat networks, consisting of one link k, connecting nodes i and node j, which both have a terminal link l connected to it. In a gas network, the quantities of interest are the link mass flow q_{ij}, terminal link mass flow $q_{i,l}$, and nodal pressure p_i. In an electrical network, they are the active power P_{ij} and reactive power Q_{ij} at the start of the

(a) Gas network.

(b) Electrical network.

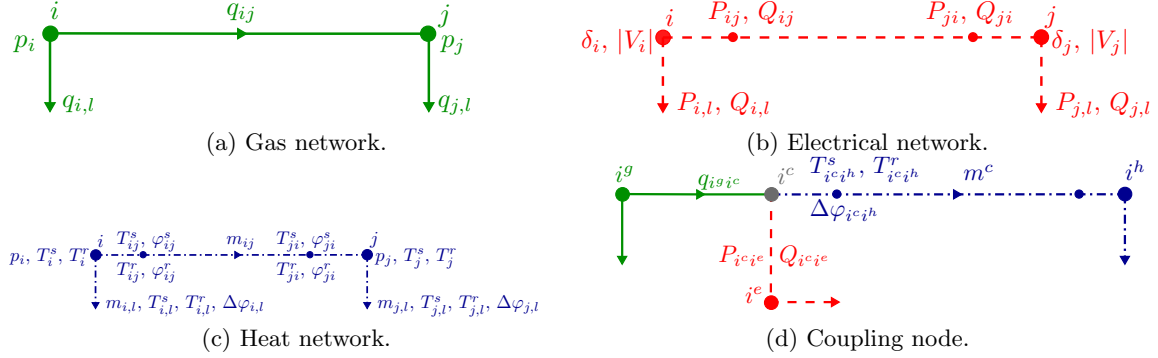(c) Heat network.

(d) Coupling node.

Figure 1: Quantities of interest for load flow simulation of energy systems, and the network elements they are associated with. Arrows on links and terminal links show defined direction of flow.

link, and P_{ji} and Q_{ji} at the end of the link, terminal link active and reactive power $P_{i,l}$ and $Q_{i,l}$, and nodal voltage amplitude $|V_i|$ and voltage angle δ_i. The terminal link powers are also called injected powers. In a heating system, hot water is transported from a source through the supply line to a heat demand. Then, cold water is transported back to the source through the return line. We assume the water flow in the return line is equal in size but opposite in direction to the flow in the supply, such that we can represent the supply line and return line with one link, and we can represent heat sources and demands with a terminal link. The quantities of interest are the link water mass flow m_{ij}, supply temperature T_{ij}^s, return temperature T_{ij}^r, and supply and return line heat powers φ_{ij}^s and φ_{ij}^r at the start of the link, and T_{ji}^s, T_{ji}^r, φ_{ji}^s and φ_{ji}^r at the end of the link, terminal link mass flow $m_{i,l}$, temperature at the supply line side $T_{i,l}^s$ and at the return line side $T_{i,l}^r$, and heat power inflow or outflow $\Delta\varphi_{i,l}$, and nodal pressure p_i, supply temperature T_i^s, and return temperature T_i^r. The heat powers on the (terminal) links are defined such that $\Delta\varphi = \varphi^s + \varphi^r$.

Figure 1d shows a multi-carrier network with a single coupling node. The coupling node itself has no nodal variables. The variables of interest for a coupling node are the link variables of the single-carrier links connected to the coupling node.

Some quantities, such as demands and a reference pressure or reference voltage, are given for load flow simulations. These are the boundary conditions (BCs) or set points of the network. Given BCs, a system of nonlinear equations has to be solved for state variables. With these state variables, all other quantities of interest in the network can be determined. As such, they are derived variables based on the state variables. For instance, in a power grid the state variables usually are the nodal voltage amplitudes and nodal voltage angles, and the derived variables are complex power through a line and injected reactive power at a generator (e.g. [9]).

The division of network variables into state variables and derived variables is not unique. In a gas network, two formulations for the LF problem are commonly used; the nodal formulation and the loop formulation (e.g. [10]). In the nodal formulation, the state variables are the nodal pressures, while the gas flows on the links are the derived variables. In the loop formulation it is the other way around, such that the state variables are the gas link flows and the nodal pressures are the derived variables. We call the vector $\boldsymbol{x}$, consisting of state variables $\boldsymbol{x^F}$ and derived variables $\boldsymbol{x^G}$, the extended state variables:

$$\boldsymbol{x} := \left(x_1^G, \ldots, x_s^G, x_1^F, \ldots, x_n^F\right)^T \tag{1}$$

7

The LF problem is concerned with solving a (non)linear system of equations for the state variables.

In optimization problems, the derived variables are also used, either in the objective function or with respect to physical limits of the energy system. We extend the standard LF equations and state variables with the derived variables and with the (non)linear equations needed to derive them, leading to the extended LF problem:

$$\boldsymbol{F}\left(\boldsymbol{x}^F\right) = \boldsymbol{0} \tag{2a}$$

$$\boldsymbol{G}\left(\boldsymbol{x}^G, \boldsymbol{x}^F\right) = \boldsymbol{0} \tag{2b}$$

Here, $\boldsymbol{F} : \mathbb{R}^n \to \mathbb{R}^n$ is the system of (non)linear steady-state load flow equations, $\boldsymbol{x}^F \in \mathbb{R}^n$ are the state variables, $\boldsymbol{G} : \mathbb{R}^{n+s} \to \mathbb{R}^s$ are additional load flow equations, and $\boldsymbol{x}^G \in \mathbb{R}^s$ are the derived variables. To solve the extended LF problem (2), the standard LF problem (2a) is solved for the state variables $\boldsymbol{x}^F$. Then, using this $\boldsymbol{x}^F$, the additional equations (2b) determine the derived variables $\boldsymbol{x}^G$.

Various formulations of the LF problem (2a) exist for a given (single-carrier) network, such as the nodal or loop formulation in a single-carrier gas network [10], or the power-mismatch or current-mismatch formulation in single-carrier power grids [14]. Moreover, the individual load flow equations within (2) can be formulated in various ways. For instance, the hydraulic flow equation used for pipes in a gas or heating network can express the pressure drop as function of flow or the other way around. These formulations influence the solvability of the optimization problem or the convergence behavior of the solvers, which we will show in Section 5.

3 Optimal Flow

An optimal flow problem (OF) finds an optimal solution to an objective function, while satisfying operational constraints or physical limits of the energy system. To ensure that the optimal solution satisfies operational constraints, the LF equations are used within OF. A solution that satisfies the operational constraints is called (physically) feasible. Solvability of OF depends on the choice of variables, the formulation of the LF equations used to model a MES, and how the LF equations are included within OF.

3.1 Objective Function

Several objective functions are used in optimization of energy systems, such as minimizing generation costs, minimizing losses, or minimizing carbon emissions. We choose to minimize total generation costs, which is commonly used in both single-carrier and multi-carrier systems (e.g. [3], [4], and [15]). We model the costs of a source as a quadratic function of its energy flow, such that the objective function is

$$f(\boldsymbol{E}) = \sum_{e \in \boldsymbol{E}} a_e + b_e e + c_e e^2 \tag{3}$$

Here, $\boldsymbol{E}$ is the vector of energy flows of the sources. For instance, for a gas source with mass flow q and gross heating value (GHV), we have $\mathrm{GHV}q \in \boldsymbol{E}$, and for a gas-fired generator that produces active power P we have $P \in \boldsymbol{E}$. The parameters a_e, b_e, and c_e specify the cost of the energy source related to energy flow e.

The sum of quadratic functions is twice-continuously differentiable. Moreover, the objective function f is convex in $\boldsymbol{E}$ for suitable parameters a_e, b_e, and c_e. Both the differentiability and convexity have several mathematical advantages (e.g. [16], [17]).

3.2 Variables and bounds

The variables $\boldsymbol{y}$ of OF can be divided into control variables $\boldsymbol{u}$ and (extended) state variables $\boldsymbol{x}$ as $\boldsymbol{y} := \left(u_1, \ldots, u_p, x_1, \ldots, x_{n+s}\right)^T$. By definition, the state variables cannot be control variables. When a design optimization problem is considered, the control variables can include design variables such as the diameter of a gas pipe. We consider an optimal flow problem, which is an operational optimization problem. The control variables are quantities in the energy system that are controllable in practice. They can include set points, which are (a subset of) the BCs of the LF problem, or model parameters such as transformer tap-ratio's [9] or dispatch factors of energy hubs [3]. Including model parameters as variables would require derivatives of the objective and constraint functions to these parameters. Since the model parameters would be part of the control variables $\boldsymbol{u}$, which are given for the LF equations, including the model parameters as variables does not change the nature of the optimization problem and the proposed framework. Therefore, we assume the model parameters are given, leaving only the BCs of LF as possible control variables.

The LF problem determines the state variables in the network, for given BCs. That is, for any $\boldsymbol{u}$, the nonlinear system (2) can be solved for $\boldsymbol{x^F}$ and $\boldsymbol{x^G}$, assuming the LF problem is well-posed. For notational simplicity, we denote the extended LF problem (2) by

$$\boldsymbol{h}\left(\boldsymbol{x};\,\boldsymbol{u}\right) := \begin{pmatrix} \boldsymbol{G}\left(\boldsymbol{x};\,\boldsymbol{u}\right) \\ \boldsymbol{F}\left(\boldsymbol{x};\,\boldsymbol{u}\right) \end{pmatrix} = \boldsymbol{0} \tag{4}$$

However, not every $\boldsymbol{u}$ results in a physically feasible extended state $\boldsymbol{x}$.

To ensure physical feasibility of the set points $\boldsymbol{u}$, bounds are imposed on network quantities. Bounds imposed on variables $\boldsymbol{y}$ are simple linear inequality constraints in the optimization problem. Bounds imposed on network quantities not in $\boldsymbol{y}$ have to be included as (non)linear inequality constraints that are a function of $\boldsymbol{y}$. These inequality constraints can be highly nonlinear.

When the energy flows of sources are part of the optimization variables, i.e. when $\boldsymbol{E} \subseteq \boldsymbol{y}$, the objective function (3) is convex in $\boldsymbol{y}$. However, when some of the energy flows in $\boldsymbol{E}$ are derived quantities that are not included in the extended state $\boldsymbol{x}$, the nonlinearity of the objective function increases, and it may no longer be convex in $\boldsymbol{y}$.

To avoid (highly) nonlinear inequality constraints, and to reduce the nonlinearity of the objective function, derived variables can be included in the extended state. On the other hand, including the derived variables in $\boldsymbol{x}$ increases the optimization space and the number of LF equations in the (extended) LF problem. Depending on the optimizer, using extended state variables instead of only the regular state variables can be beneficial.

3.3 Two Problem Formulations

The optimization problem determines a solution that minimizes the objective function, while satisfying the LF problem and while staying within the feasibility limits. We consider two ways to formulate the optimal flow (OF) problem, which we call formulation I and formulation II. Formulation I includes the LF equations as equality constraints, while formulation II includes them as subsystem.

3.3.1 Formulation I: LF as equality constraints

The most straightforward way to satisfy the LF equations during optimization is to include them as equality constraints directly, and optimize over the combined control and (extended) state variables (as is done in e.g. [3], [4], and [15]). This gives formulation I of the OF problem:

$$\min_{\boldsymbol{x},\,\boldsymbol{u}}\quad f\left(\boldsymbol{x},\,\boldsymbol{u}\right) \tag{5a}$$

$$\text{s.t}\quad \boldsymbol{h}\left(\boldsymbol{x};\,\boldsymbol{u}\right)=\boldsymbol{0} \tag{5b}$$

$$\boldsymbol{\gamma}\left(\boldsymbol{x},\,\boldsymbol{u}\right)\geq\boldsymbol{0} \tag{5c}$$

$$\boldsymbol{u}^{lb}\leq\boldsymbol{u}\leq\boldsymbol{u}^{ub} \tag{5d}$$

$$\boldsymbol{x}^{lb}\leq\boldsymbol{x}\leq\boldsymbol{x}^{ub} \tag{5e}$$

Here, $f:\mathbb{R}^{n+s+p}\to\mathbb{R}$ is the objective function (3), $\boldsymbol{u}\in\mathbb{R}^{p}$ is the vector of control variables, $\boldsymbol{x}\in\mathbb{R}^{n+s}$ is the vector of extended state variables (1), $\boldsymbol{h}:\mathbb{R}^{n+s+p}\to\mathbb{R}^{n+s}$ are the equality constraints given by the extended system of LF equations (4), $\boldsymbol{u}^{lb}$ and $\boldsymbol{u}^{ub}$ are the lower and upper bounds for the control variables, $\boldsymbol{x}^{lb}$ and $\boldsymbol{x}^{ub}$ are the lower and upper bounds for the extended state variables, and $\boldsymbol{\gamma}:\mathbb{R}^{n+s+p}\to\mathbb{R}^{m}$ are inequality constraints representing the bounds for any network quantities not included in $\boldsymbol{y}$.

3.3.2 Formulation II: LF as subsystem

Another way to formulate the optimization problem is to apply (nonlinear) elimination of variables and constraints (e.g. [16], [17]). We eliminate the extended state variables $\boldsymbol{x}$ using the LF equations (4), to get an optimization over the control variables $\boldsymbol{u}$ only. This gives formulation II of the OF problem:

$$\min_{\boldsymbol{u}}\quad f\left(\boldsymbol{x}\left(\boldsymbol{u}\right),\,\boldsymbol{u}\right) \tag{6a}$$

$$\text{s.t}\quad \boldsymbol{u}^{lb}\leq\boldsymbol{u}\leq\boldsymbol{u}^{ub} \tag{6b}$$

$$\boldsymbol{g}\left(\boldsymbol{x}\left(\boldsymbol{u}\right),\,\boldsymbol{u}\right)\geq\boldsymbol{0} \tag{6c}$$

$$\text{with}\quad \boldsymbol{g}\left(\boldsymbol{x}\left(\boldsymbol{u}\right),\,\boldsymbol{u}\right)=\begin{pmatrix}\boldsymbol{\gamma}\left(\boldsymbol{x}\left(\boldsymbol{u}\right),\,\boldsymbol{u}\right)\\ \boldsymbol{x}\left(\boldsymbol{u}\right)-\boldsymbol{x}^{lb}\\ \boldsymbol{x}^{ub}-\boldsymbol{x}\left(\boldsymbol{u}\right)\end{pmatrix} \tag{6d}$$

The relation $\boldsymbol{x}\left(\boldsymbol{u}\right)$ is implicitly given by the extended LF problem (4). That is, for any given $\boldsymbol{u}$, the (extended) state $\boldsymbol{x}$ satisfies the LF equations by solving $\boldsymbol{x}$ from (4).

3.3.3 Comparison

If bounds are only imposed on network quantities that are included in $\boldsymbol{y}$, then $m=0$, (5c) is not included in optimization problem (5), and $\boldsymbol{\gamma}$ is not included in (6d). Similarly, bounds do not have to be imposed on all variables in $\boldsymbol{y}$. Suppose bounds are imposed on $\tilde{p}\leq p$ of the control variables and on $\tilde{n}+\tilde{s}\leq n+s$ of the extended state variables. Then (5d) and (6b) consist of $\tilde{p}$ bounds, which are $2\tilde{p}$ linear inequality constraints, and (5e) consists of $\tilde{n}+\tilde{s}$ bounds or $2\tilde{n}+2\tilde{s}$ linear inequality constraints. Furthermore, $\boldsymbol{g}:\mathbb{R}^{n+s+p}\to\mathbb{R}^{m+2\tilde{n}+2\tilde{s}}$ such that (6c) consists of $m+2\tilde{n}+2\tilde{s}$ (non)linear inequality constraints.

10

Formulations I and II have several advantages and disadvantages. Formulation II has a smaller optimization space, due to the elimination of extended state variables. However, this elimination increases the nonlinearity of the inequality constraints and objective function, and the linear bounds (5e) are turned into (non)linear inequality constraints (6c). Moreover, elimination of variables using nonlinear equations may result in errors ([17] pp. 426–428). Using nonlinear inequality constraints $\boldsymbol{\gamma}$ in (5c) or in (6d), instead of including derived variables in the extended state variables, is an example of (nonlinear) elimination of variables as well. This type of elimination is commonly used in optimal power flow problems (e.g. [9]).

An advantage of formulation II is that the extended LF problem (4) is solved separately. The LF problem can be delegated to a dedicated LF solver, instead of having the optimizer itself solve the LF problem. A user solving the optimization problem does not need to have access to the LF model; they only need access to the output and be able to set the input. This can be an advantage, especially when optimizing a multi-carrier system, where the operator of each carrier might have their own LF solver. Moreover, dedicated LF solvers might be more efficient at solving the LF problem than an optimizer. However, the LF problem needs to be solved (at least) once per iteration of the optimization algorithm used to solve (6). This might increase the total computation time of the optimizer for formulation II compared with formulation I, depending on the efficiency of the dedicated LF solver. On the other hand, this means the LF equations are satisfied at every iteration of the optimizer. Depending on the optimizer, equality constraints are not satisfied at every iteration, such that the LF equations are not always satisfied when using optimization problem (5). Therefore, problem (6) can be preferred to (5) if feasibility has to be ensured.

The same quadratic objective function is used in both problems. If the objective function depends on $\boldsymbol{x}$, then it might have some nonlinear dependency on $\boldsymbol{u}$, other than quadratic, in problem (6). The (in)equality constraints (5b) and (5c) generally are nonlinear in $\boldsymbol{y}$, while (5d) and (5e) are linear inequality constraints. If bounds are imposed on variables in $\boldsymbol{y}$ only, such that (5c) is not included, problem (5) is an optimization problem with nonlinear equality constraints and linear inequality constraints. If (5c) is included, problem (5) is an optimization problem with nonlinear equality and nonlinear inequality constraints. The inequality constraints (6c) generally are nonlinear in $\boldsymbol{u}$, regardless of whether $\boldsymbol{\gamma}$ is included or not. Problem (6) is an optimization problem with nonlinear inequality constraints, but has no equality constraints. Both problems (5) and (6) are nonlinearly constrained optimization problems.

Since the two formulations have advantages and disadvantages, we compare the two formulations using some example multi-carrier networks.

4 Solving the Optimal Flow Problem

OF problems (5) and (6) are nonlinear, (in)equality constrained, multivariable optimization problems. It is generally not possible to determine analytically if the first-order, or KKT, and second-order optimality conditions are met. Moreover, when the objective function is concave, or when the (in)equality constraints are nonlinear, which is the case for most load flow equations, the solution space might be non-convex. Hence, we use numerical solvers to approximate an optimal solution.

4.1 Optimizers

To solve problems (5) and (6) we consider three solvers used for nonlinearly constrained optimization problems: The 'trust-constr' (t-c) and 'SLSQP' methods from SciPy [18], and IPOPT [19].

The trust-constr method is a trust-region interior-point method for large-scale nonlinear optimization problems, based on the algorithm developed in [20]. Inequality constraints are handled by introducing a barrier function. The resulting barrier subproblems are solved using an adapted version of the Byrd-Omojokun Trust-Region Sequential Quadratic Programming (SQP) Method ([17] p. 549). The trust-constr method is a projected Lagrangian method.

The SLSQP method is a sequential least squares programming method, based on the algorithm developed in [21]. It is a projected Lagrangian method, where a sequence of linearly constrained quadratic programming (QP) subproblems is created. The Hessian of the Lagrangian is factorized, turning the QP problem into a least-squares problem. Hence, a sequence of least-squares subproblems is solved. Unlike the trust-constr method, the SLSQP method does not require the Hessian of the Lagrangian.

IPOPT is a primal-dual interior-point method for large-scale nonlinear optimization problems, using the algorithm developed in [19]. Like the trust-constr method, inequality constraints are handled by introducing a barrier function. These barrier subproblems are solved by applying Newton's method to the system of primal-dual equations. The search directions for the next iterate are determined by linearizing these primal-dual equations. The step sizes are determined by a backtracking line-search procedure, which is a variant of a filter method, to ensure global convergence.

4.2 Scaling

Badly scaled optimization problems cause convergence issues for the optimizer [22]. In energy systems, especially in multi-carrier systems, the variables and model parameters can differ several orders of magnitude. For instance, gas flow $q \sim 1\,\mathrm{kg/s}$ while active power $P \sim 10^7\,\mathrm{W}$. Hence, the optimization problem for a MES is usually scaled badly.

Scaling does not influence the iterates of Newton's method, which we use to solve the LF problem [22, 23]. However, scaling might influence the iterates of an optimizer [22]. For instance, scaling changes the steepest-descent direction.

We consider per unit scaling and matrix scaling [23]. Per unit scaling scales all variables and model parameters directly. This scaling is generally used in LF and OF problems in power grids. Matrix scaling does not scale the model parameters, but scales the variables and systems of equations using matrix multiplication. To scale the objective function using per unit scaling, the parameters a_e, b_e, and c_e in (3) are also scaled. When using matrix scaling, we scale the objective function with a chosen base value instead.

4.3 Additional steps for formulation II

Formulation II of the OF problem includes the state variables $\boldsymbol{x}$ and associated LF equations as a subsystem, which requires additional steps in the optimization algorithm.

The trust-constr method uses the Hessian H of the objective function. For the general objective function (3) the Hessian is a constant diagonal matrix. This is also true for problem (5) in formulation I, where $e \in \boldsymbol{y}$ for all $e \in \boldsymbol{E}$, such that

$$H_{ij} := \frac{\partial^2 f}{\partial y_i \partial y_j} = \begin{cases} 2c_e, & y_i = y_j := e \in \boldsymbol{E} \\ 0, & \text{otherwise} \end{cases} \tag{7}$$

In formulation II, where $\boldsymbol{x}$ depends (implicitly) on $\boldsymbol{u}$, the Hessian is no longer constant if any of the energy flows e in the objective is part of $\boldsymbol{x}$ instead of $\boldsymbol{u}$. Therefore, we let trust-constr determine

12

the Hessian numerically for formulation II.

The considered optimizers use the gradient of the objective and the Jacobian of the (in)equality constraints. For formulation II, the gradient and Jacobian can be determined by a direct or an adjoint approach (e.g. [24] and [25]). The direct approach is also called the forward approach, and the adjoint approach is also called the backward approach. The gradient of the objective (6a) and the Jacobian of the inequality constraints (6c) to the control variables are given by

$$\frac{df}{du} = \frac{\partial f}{\partial x}\frac{dx}{du} + \frac{\partial f}{\partial u} \tag{8a}$$

$$\frac{dg}{du} = \frac{\partial g}{\partial x}\frac{dx}{du} + \frac{\partial g}{\partial u} \tag{8b}$$

For notational simplicity, we denote partial derivatives by a subscript, e.g. $\boldsymbol{g_u} := \frac{\partial g}{\partial u}$. Furthermore, we define $v := \frac{dx}{du}$, such that $v \in \mathbb{R}^{n+s} \times \mathbb{R}^p$. Using the extended LF problem (4) we have:

$$\boldsymbol{h_x} v = -\boldsymbol{h_u} \tag{9}$$

4.3.1 Formulation II.A: Direct approach

In the direct or forward approach, (8) is determined using (9) directly. That is, the gradient and the Jacobian are given by

$$\frac{df}{du} = f_{\boldsymbol{x}} v + f_{\boldsymbol{u}} \tag{10a}$$

$$\frac{dg}{du} = \boldsymbol{g_x} v + \boldsymbol{g_u} \tag{10b}$$

$$\text{where } \boldsymbol{h_x} v = -\boldsymbol{h_u} \tag{10c}$$

Here, v is determined by solving (10c). Hence, formulation II.A requires solving p linear systems of size $(n+s) \times (n+s)$ any time $\frac{df}{du}$ or $\frac{dg}{du}$ is calculated.

4.3.2 Formulation II.B: Adjoint approach

In the adjoint or backward approach, we introduce $\boldsymbol{\lambda}^T := f_{\boldsymbol{x}} \boldsymbol{h_x}^{-1}$ and $\mu^T := \boldsymbol{g_x} \boldsymbol{h_x}^{-1}$ to determine (8). With these definitions of $\boldsymbol{\lambda} \in \mathbb{R}^{n+s}$ and $\mu \in \mathbb{R}^{n+s} \times \mathbb{R}^{m+2\tilde{n}+2\tilde{s}}$, we have $f_{\boldsymbol{x}} v = -\boldsymbol{\lambda}^T \boldsymbol{h_u}$ and $\boldsymbol{g_x} v = -u^T \boldsymbol{h_u}$. The gradient and the Jacobian are then given by

$$\frac{df}{du} = -\boldsymbol{\lambda}^T \boldsymbol{h_u} + f_{\boldsymbol{u}} \tag{11a}$$

$$\frac{dg}{du} = -\mu^T \boldsymbol{h_u} + \boldsymbol{g_u} \tag{11b}$$

$$\text{where } \boldsymbol{h_x}^T \boldsymbol{\lambda} = f_{\boldsymbol{x}}^T \tag{11c}$$

$$\boldsymbol{h_x}^T \mu = \boldsymbol{g_x}^T \tag{11d}$$

Here, $\boldsymbol{\lambda}$ and μ are determined by solving (11c) and (11d) respectively. Hence, formulation II.A requires solving $1 + m + 2\tilde{n} + 2\tilde{s}$ linear systems of size $(n+s) \times (n+s)$ any time $\frac{df}{du}$ or $\frac{dg}{du}$ is calculated.

4.3.3 Comparison

The direct approach requires solving (10c), which are p linear systems of size $(n + s) \times (n + s)$. The adjoint approach requires solving (11c) and (11d), which are $1 + m + 2\tilde{n} + 2\tilde{s}$ linear systems of size $(n + s) \times (n + s)$. Since the linear systems in both approaches have the same size, the adjoint approach might be more efficient than the direct approach if $p > 1 + m + 2\tilde{n} + 2\tilde{s}$. In other words, the adjoint approach might be faster if the number of control variables is large compared to the number of (nonlinear) inequality constraints. For optimization problems of energy systems, this is generally not the case. With our assumptions, and imposing bounds on most of the extended state variables, we indeed have $p < 1 + m + 2\tilde{n} + 2\tilde{s}$. Therefore, we expect that the direct approach is more efficient than the adjoint approach.

4.3.4 Load flow as subproblem

Whenever one of the extended state variables $\boldsymbol{x}(\boldsymbol{u})$ is needed while solving problem (6), the extended LF problem (4) would need to be solved. Since $\boldsymbol{x}(\boldsymbol{u})$ might be used several times per iteration of the optimizer, the system (4) might be solved multiple times per optimizer iteration. To increase efficiency, we store the values $\boldsymbol{x}(\boldsymbol{u})$. Furthermore, the extended LF problem (4) is only solved to determine a new $\boldsymbol{x}(\boldsymbol{u})$ if $\boldsymbol{u}$ has changed significantly since the last solve, or if the LF equations with the current $\boldsymbol{x}$ are not satisfied within a desired tolerance. Suppose $\boldsymbol{x}^k$ and $\boldsymbol{u}^i$ are the previous values of the extended state and control variables, and $\boldsymbol{u}^{i+1}$ are the current control variables. The extended LF problem (4) is only solved if

$$||\boldsymbol{u}^{i+1} - \boldsymbol{u}^i||_2 > \tau \tag{12a}$$

$$\text{or } ||\boldsymbol{h}\left(\boldsymbol{x}^k, \boldsymbol{u}^i\right)||_2 > \varepsilon \tag{12b}$$

with τ and ε tolerances. We store $||\boldsymbol{h}(\boldsymbol{x}, \boldsymbol{u})||_2$ any time (4) is solved to evaluate (12b) without having to recalculate the LF equations.

5 Comparison of formulations and solvers of the optimal flow problem

Combining all possible ways described in Sections 3 and 4 to formulate and solve the OF problem leads to multiple combinations. To compare these various formulations and aspects of the optimization problem, we optimize two different MESs. We mainly compare the various formulations and aspects based on the efficiency of the optimizer. That is, first we determine if an optimal solution is found. Then, the number of iterations and function calls to the objective functions required by the optimizer are used as a measure for efficiency.

We compare formulation I and formulation II, i.e. the way that LF is incorporated into OF, for both MESs. Additionally, for each MES we focus on some of the formulations and aspects of solving the OF problem. Scaling greatly improves the convergence of the optimizers for the LF problem. Hence, we only consider the scaled OF problem.

The coupling of first MES is modeled in two different ways, giving two multi-carrier network representations for the same MES. For both versions, we use a single formulation of the LF equations. Bounds are imposed on all variables $\boldsymbol{y}$ or on the control variables $\boldsymbol{u}$ only. Within the optimizers, the inequality constraints are taken as hard constraints or as soft constraints. With hard constraints,

each iteration of the optimizer must satisfy all inequality constraints. With soft constraints, iterates are allowed to violate the inequality constraints, but the final solution must satisfy all constraints. We consider both, since hard constraints might help keep the iterates feasible. Hence, we use this MES to focus on the inequality constraints.

The second MES is represented by one multi-carrier network, but we use multiple formulation of the LF equations. We consider two options in the gas part and two in the heat part. Bounds are imposed on (most) variables $\boldsymbol{y}$. We look at the effect of imposing bounds on some derived variables. These variables might not be included in $\boldsymbol{y}$, depending on the formulation of the system of LF equations. Furthermore, we compare the two methods of scaling described in Section 4.2. Finally, the number of demands in each carrier of this MES can be changed, giving multi-carrier networks of various sizes. Hence, this MES focuses on the effect of the LF formulation on OF and on scaling.

5.1 Costs of energy sources

The cost parameters a_e, b_e, and c_e in the objective function (3) are chosen to represent the variable operation and maintenance costs of the energy sources. The focus of this research is on the mathematical formulation of the optimization problem, and the inclusion of the load flow equations within an optimization framework. As such, the values of the cost parameters a_e, b_e, and c_e are chosen to be realistic, but are not meant to be accurate values of any specific energy source.

For non-coupling sources or (external) grid connections, we take $a_e = c_e = 0$ for all carriers, $b_{gas} = 15 \, €/(\mathrm{MW\,h})$ for gas, $b_{elec.} = 40 \, €/(\mathrm{MW\,h})$ for electricity, and $b_{heat} = 16 \, €/(\mathrm{MW\,h})$ for heat.

The operational costs of the coupling components are based on the produced energy. A combined heat and power plant (CHP) produces both electricity and heat, but the heat is 'waste' from the production of electricity, such that it is considered free. We take $b_{CHP} = 5 \, €/(\mathrm{MW\,h})$ and $c_{CHP} = 0.05 \, €/(\mathrm{MW^2\,h})$, and $b_{GG} = 2 \, €/(\mathrm{MW\,h})$ and $c_{GG} = 0.02 \, €/(\mathrm{MW^2\,h})$, for the active power P produced by a CHP and a gas-fired generator (GG), and $b_{GB} = 1 \, €/(\mathrm{MW\,h})$ and $c_{GB} = 0.01 \, €/(\mathrm{MW^2\,h})$, for the heat power $\Delta\varphi$ produced by a gas-boiler (GB).

5.2 MES 1: Effect of inequality constraints

The first MES is a small system first introduced in [26], where a gas, electricity, and heat network are connected by several coupling components. It was later adapted to use the energy hub (EH) approach in [12]. We model the energy system by two different networks, as described in [13]. Figure 2 shows the topology of the two networks. Network 1, see Figure 2a, uses a GG, a GB, and a CHP for the coupling. Network 2, see Figure 2b, uses EHs. In both networks, link 1^g–3^g represents a compressor, while the other gas links represent pipes. Nodes 1 and 2 are sinks in all single-carrier networks, and node 0^g has an external source. See [13] for further details and the specific LF equations used.
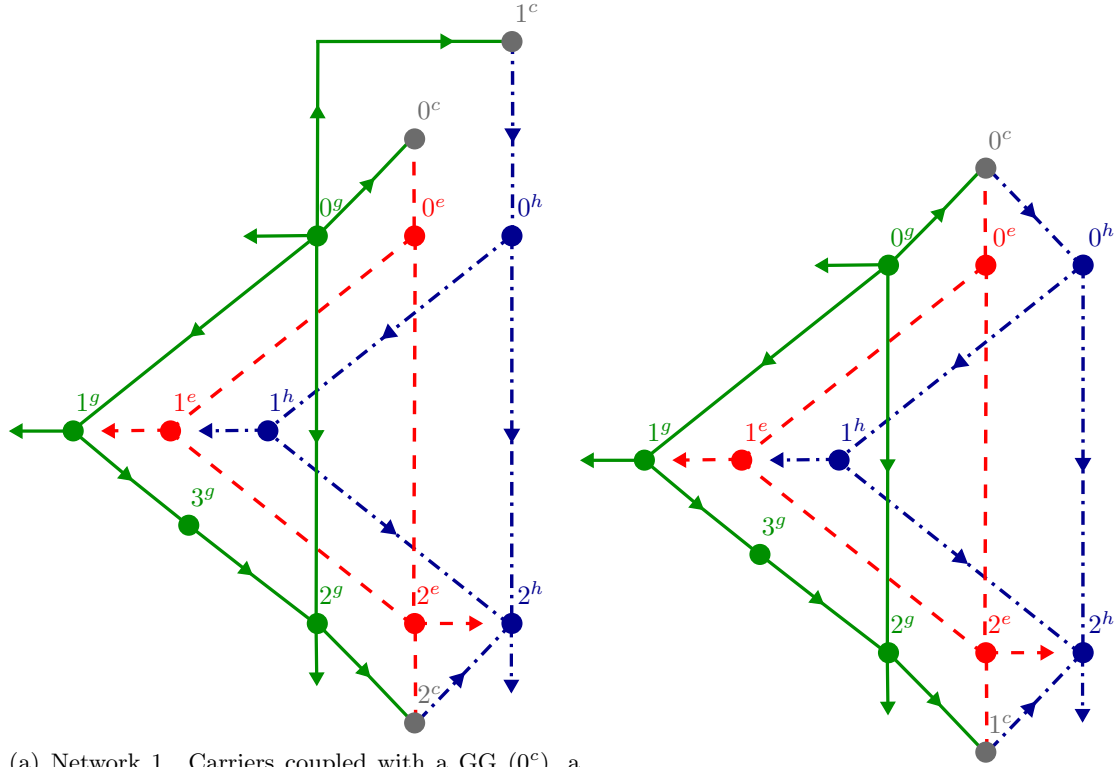
(a) Network 1. Carriers coupled with a GG (0^c), a GB (1^c), and a CHP (2^c).

(b) Network 2. Carriers coupled with EHs.

Figure 2: MES network topologies, see also [13]. Network (a) is based on [26], network (b) is based on [12]. Arrows on links and terminal links show defined direction of flow.

Table 1: Boundary conditions for steady-state LF for the networks in Figure 2.

(a) Network 1. Coupled with a GG, a GB, and a CHP.

Node	Node type	Specified	Unknown
0^g	ref.	p^g	q
1^g	load	q	p^g
2^g	ref. load	p^g, q	-
3^g	load	$q = 0$	p^g
0^e	PQVδ	$P, Q, |V|, \delta$	-
1^e	load	P, Q	$|V|, \delta$
2^e	PQV	$P, Q, |V|$	δ
0^h	ref.	p^h, $m = 0$	T^r, T^s
1^h	load (sink)	$T^r_{1,0}, \Delta\varphi_{1,0} > 0$	$T^r, T^s, p^h, m_{1,0}$
2^h	load (sink) ref.	$T^r_{2,0}, \Delta\varphi_{2,0} > 0, p^h$	$T^s, T^r, m_{2,0}$
0^c	standard	-	-
1^c	temp.	$T^s_{1^c0^h}$	-
2^c	temp.	$T^s_{2^c2^h}$	-

(b) Network 2. Coupled with EHs.

Node	Node type	Specified	Unknown
0^g	ref.	p^g	q
1^g	load	q	p^g
2^g	load	q	p^g
3^g	load	$q = 0$	p^g
0^e	PQVδ	$P, Q, |V|, \delta$	-
1^e	load	P, Q	$|V|, \delta$
2^e	PQV	$P, Q, |V|$	δ
0^h	ref.	p^h, $m = 0$	T^r, T^s
1^h	sink	$T^r_{1,0}, \Delta\varphi_{1,0} > 0$	$T^r, T^s, p^h, m_{1,0}$
2^h	sink	$T^r_{2,0}, \Delta\varphi_{2,0} > 0$	$T^r, T^s, p^h, m_{2,0}$
0^c	temp.	$T^s_{0^c0^h}$	-
1^c	temp.	$T^s_{1^c2^h}$	-

16

5.2.1 Problem Formulations

Both networks have only one external source, connected to node 0^g. The electrical and heat powers are produced by the couplings. The energy vector $\boldsymbol{E}$ of the objective function (3) is

$$\boldsymbol{E} = \left(-\mathrm{GHV}q_{0,0},\, P_{0^c0^e},\, P_{2^c2^e},\, \Delta\varphi_{1^c0^h}\right)^T, \quad \text{for network 1} \tag{13a}$$

$$\boldsymbol{E} = \left(-\mathrm{GHV}q_{0,0},\, P_{0^c0^e},\, P_{1^c2^e},\, \Delta\varphi_{0^c0^h}\right)^T, \quad \text{for network 2} \tag{13b}$$

Table 1 gives the BCs of both networks used in the LF equations. The BCs in network 1 are slightly different from those in network 2, due to the different coupling components. We take some of these known variables as control variables in the OF problem:

$$\boldsymbol{u} = \left(p_2^g,\, |V_2|,\, p_2^h,\, T_{2^c2^h}^s\right)^T, \quad \text{for network 1} \tag{14a}$$

$$\boldsymbol{u} = \left(|V_2|,\, T_{1^c2^h}^s\right)^T, \quad \text{for network 2} \tag{14b}$$

The choice for control variables is different for the two networks, since the BCs used in LF are different.

For the LF problem, we use the full formulation in the gas network, and the terminal link flow formulation in the heat network. See Section 5.3.1 for the description of these formulations. The extended state variables for network 1 are then:

$$\boldsymbol{x}^G = \left(q_{0,0}\right) \tag{15a}$$

$$\boldsymbol{x}^{F,g} = \left(q_{01},\, q_{02},\, q_{32},\, q_{13},\, p_1^g,\, p_3^g\right)^T \tag{15b}$$

$$\boldsymbol{x}^{F,e} = \left(\delta_1,\, \delta_2,\, |V_1|\right)^T \tag{15c}$$

$$\boldsymbol{x}^{F,h} = \left(m_{01},\, m_{02},\, m_{12},\, m_{1,0},\, m_{2,0},\, p_1^h,\, T_0^s,\, T_1^s,\, T_2^s,\, T_0^r,\, T_1^r,\, T_2^r\right)^T \tag{15d}$$

$$\boldsymbol{x}^{F,c} = \left(q_{0^g0^c},\, q_{0^g1^c},\, q_{2^g2^c},\, P_{0^c0^e},\, P_{2^c2^e},\, Q_{0^c0^e},\, Q_{2^c2^e},\, m_{1^c0^h},\, m_{2^c2^h},\, \Delta\varphi_{1^c0^h},\, \Delta\varphi_{2^c2^h}\right)^T \tag{15e}$$

and the extended state variables for network 2 are:

$$\boldsymbol{x}^G = \left(q_{0,0}\right) \tag{16a}$$

$$\boldsymbol{x}^{F,g} = \left(q_{01},\, q_{02},\, q_{32},\, q_{13},\, p_1^g,\, p_2^g,\, p_3^g\right)^T \tag{16b}$$

$$\boldsymbol{x}^{F,e} = \left(\delta_1,\, \delta_2,\, |V_1|\right)^T \tag{16c}$$

$$\boldsymbol{x}^{F,h} = \left(m_{01},\, m_{02},\, m_{12},\, m_{1,0},\, m_{2,0},\, p_1^h,\, p_2^h,\, T_0^s,\, T_1^s,\, T_2^s,\, T_0^r,\, T_1^r,\, T_2^r\right)^T \tag{16d}$$

$$\boldsymbol{x}^{F,c} = \left(q_{0^g0^c},\, q_{2^g1^c},\, P_{0^c0^e},\, P_{1^c2^e},\, Q_{0^c0^e},\, Q_{1^c2^e},\, m_{0^c0^h},\, m_{1^c2^h},\, \Delta\varphi_{0^c0^h},\, \Delta\varphi_{1^c2^h}\right)^T \tag{16e}$$

Hence, there are 37 variables for network 1, consisting of 32 state variables $\boldsymbol{x}^F$, 1 derived variable $\boldsymbol{x}^G$, and 4 control variables $\boldsymbol{u}$, and 36 variables for network 2, consisting of 33 state variables $\boldsymbol{x}^F$, 1 derived variable $\boldsymbol{x}^G$, and 2 control variables $\boldsymbol{u}$.

The extended LF problem (4) is not solvable (for a physically feasible solution) for all values of $\boldsymbol{u}$. The bounds imposed on $\boldsymbol{u}$ are chosen such that the LF problem is solvable. This requires relatively tight bounds, especially for p_2^g and p_2^h.

We can impose bounds on $\boldsymbol{u}$ only, or on the extended state variables $\boldsymbol{x}$ as well. We solve the OF problem in both cases, with bounds on $\boldsymbol{u}$ only, and with bounds on $\boldsymbol{y}$. Moreover, we consider hard and soft inequality constraints within the optimizer.

This gives a total of 12 different formulations and solution methods of the OF problem for both network representations of this MES. That is, we use formulation I (5) for the OF problem, including the LF equations as equality constraints, or we use formulation II (6), eliminating LF equations. For the latter, we can use the direct approach II.A or the adjoint approach II.B when solving the optimization problem. For each of these, we impose bounds on u or on y, and we use soft or hard bound within the optimizers. In addition to these 12 options, we use t-c, SLSQP, or IPOPT as optimizer, see Section 4.1.

Table 2 gives the number and size of the linear systems (10c) and (11c)–(11d) for formulation II.A en II.B. Using soft or hard constraints does not change the system size. For both formulation II.A and II.B, the size of the linear systems is equal, since h_x is square. If bounds are imposed on u only, there are no (nonlinear) inequality constraints on $x(u)$, such that the OF problem is given by (6a)–(6b). In that case, only (8a) is needed, such that only (11c) needs to be solved for formulation II.B. Hence, formulation II.B requires solving fewer linear systems than formulation II.A when bounds are imposed on u, while formulation II.B requires solving significantly more linear systems than formulation II.A when bounds are imposed on y.

Table 2: Number and size of the linear systems (10c) and (11c)–(11d) for formulation II.A en II.B for network 1 (a) and network 2 (b).

(a) Network 1. Coupled with a GG, GB, and CHP.

bounds on	OF form.	# lin. sys.	size lin. sys.
u	II.A	4	33×33
	II.B	1	33×33
y	II.A	4	33×33
	II.B	67	33×33

(b) Network 2. Coupled with EHs.

bounds on	OF form.	# lin. sys.	size lin. sys.
u	II.A	2	34×34
	II.B	1	34×34
y	II.A	2	34×34
	II.B	69	34×34

5.2.2 Results

We set the tolerance for the OF problem, for the extended LF problem ε, and τ to 10^{-6}, and use matrix scaling to scale the problem. The maximum number of iterations for the optimizers is 40, and 10 for Newton's method to solve the extended LF problem (4) within formulation II. We have found that the optimizers were unlikely to find a solution if it did not find one within these 40 iterations.

Tables 3 and 4 give the results for network 1 and 2 respectively. A '-' indicates the optimizer is unable to find a solution for that particular case. The columns # iters and # f give the number of iterations and number of calls to the objective function of the optimizer respectively. The last column gives the error of the LF equations $||F||_2$ for the found optimal solution.

First, we compare the optimizers. For network 1, t-c and IPOPT are not able to find a solution for any of the options, while SLSQP finds a solution for all options. For network 2, IPOPT finds a solution for all options, and t-c and SLSQP for all options using formulation II only.

We consider both soft and hard constraints, since hard constraints might avoid convergence issues due to infeasible iterates. In various examples, we have seen that using appropriate values for the bounds and using a reasonable initial guess are more effective to ensure feasible iterates than imposing hard constraints. Tables 3 and 4 show this is also the case for this MES. There is no case for which any of the optimizers find a solution with hard constraints but not with soft constraints.

18

Table 3: Information on optimizers of the optimal flow problem for network 1, using matrix scaling.

bounds on	constraints	OF form.	# iters			# f			$\|\boldsymbol{F}\|_2$		
			t-c	SLSQP	IPOPT	t-c	SLSQP	IPOPT	t-c	SLSQP	IPOPT
$\boldsymbol{u}$	soft	I	-	21	-	-	32	-	-	$4.782 \cdot 10^{-7}$	-
		II.A	-	15	-	-	38	-	-	$2.674 \cdot 10^{-10}$	-
		II.B	-	15	-	-	38	-	-	$2.674 \cdot 10^{-10}$	-
	hard	I	-	21	-	-	32	-	-	$4.782 \cdot 10^{-7}$	-
		II.A	-	15	-	-	38	-	-	$2.674 \cdot 10^{-10}$	-
		II.B	-	15	-	-	38	-	-	$2.674 \cdot 10^{-10}$	-
$\boldsymbol{y}$	soft	I	-	21	-	-	32	-	-	$4.782 \cdot 10^{-7}$	-
		II.A	-	9	-	-	42	-	-	$6.606 \cdot 10^{-7}$	-
		II.B	-	8	-	-	42	-	-	$1.312 \cdot 10^{-7}$	-
	hard	I	-	21	-	-	32	-	-	$4.782 \cdot 10^{-7}$	-
		II.A	-	9	-	-	42	-	-	$6.606 \cdot 10^{-7}$	-
		II.B	-	8	-	-	42	-	-	$1.312 \cdot 10^{-7}$	-

Table 4: Information on optimizers of the optimal flow problem for network 2, using matrix scaling.

bounds on	constraints	OF form.	# iters			# f			$\|\boldsymbol{F}\|_2$		
			t-c	SLSQP	IPOPT	t-c	SLSQP	IPOPT	t-c	SLSQP	IPOPT
$\boldsymbol{u}$	soft	I	-	-	15	-	-	16	-	-	$3.744 \cdot 10^{-9}$
		II.A	20	6	10	14	7	11	$2.696 \cdot 10^{-7}$	$8.532 \cdot 10^{-7}$	$5.605 \cdot 10^{-7}$
		II.B	20	6	10	14	7	11	$2.696 \cdot 10^{-7}$	$8.532 \cdot 10^{-7}$	$5.605 \cdot 10^{-7}$
	hard	I	-	-	15	-	-	16	-	-	$4.232 \cdot 10^{-9}$
		II.A	16	6	10	10	7	11	$2.723 \cdot 10^{-7}$	$8.532 \cdot 10^{-7}$	$5.605 \cdot 10^{-7}$
		II.B	16	6	10	10	7	11	$2.723 \cdot 10^{-7}$	$8.532 \cdot 10^{-7}$	$5.605 \cdot 10^{-7}$
$\boldsymbol{y}$	soft	I	30	-	14	30	-	15	$1.944 \cdot 10^{-8}$	-	$3.817 \cdot 10^{-8}$
		II.A	24	9	9	27	22	10	$7.465 \cdot 10^{-7}$	$4.268 \cdot 10^{-8}$	$4.163 \cdot 10^{-8}$
		II.B	24	9	9	27	22	10	$7.465 \cdot 10^{-7}$	$4.257 \cdot 10^{-8}$	$4.163 \cdot 10^{-8}$
	hard	I	26	-	14	26	-	15	$1.124 \cdot 10^{-6}$	-	$3.817 \cdot 10^{-8}$
		II.A	15	9	9	9	22	10	$1.455 \cdot 10^{-7}$	$4.268 \cdot 10^{-8}$	$4.163 \cdot 10^{-8}$
		II.B	15	9	9	9	22	10	$1.455 \cdot 10^{-7}$	$4.257 \cdot 10^{-8}$	$4.163 \cdot 10^{-8}$

That is, there is no advantage to using hard bounds.

Then, we consider the bounds. For network 1 and formulation I, there is no difference between bounds on $\boldsymbol{u}$ or $\boldsymbol{y}$. For network 1 and formulation II, bounds on $\boldsymbol{y}$ reduces the number of iterations. For network 2 and formulation I, t-c is only able to find a solution when bounds are imposed on $\boldsymbol{y}$. For network 2 and formulation II, imposing bounds on $\boldsymbol{u}$ requires more iterations for SLSQP. The other optimizers seem to be less affected by this in this case. Hence, if bounds should be imposed on $\boldsymbol{u}$ or on $\boldsymbol{y}$ depends on the network and the optimizer.

Finally, we consider the inclusion of the LF equations in the OF problem, that is, we compare formulation I with formulation II. Figure 3 gives the error of the LF equations at every iteration of the optimizer, for the OF problem of network 1 with soft bounds on $\boldsymbol{y}$ using SLSQP, and illustrates the difference between the two formulations. As stated in Section 3.3.3, Figure 3 shows that the LF equations are satisfied at every iteration when using formulation II, while this is not the case for formulation I.Table 4 shows that there are cases where a solution cannot be found using formulation I while it is found using formulation II. However, there are also cases where both formulation I and II result in a solution. Tables 3 and 4 both show that formulation II requires fewer iterations than formulation I, for all considered cases. Furthermore, formulation I gives a different optimal solution
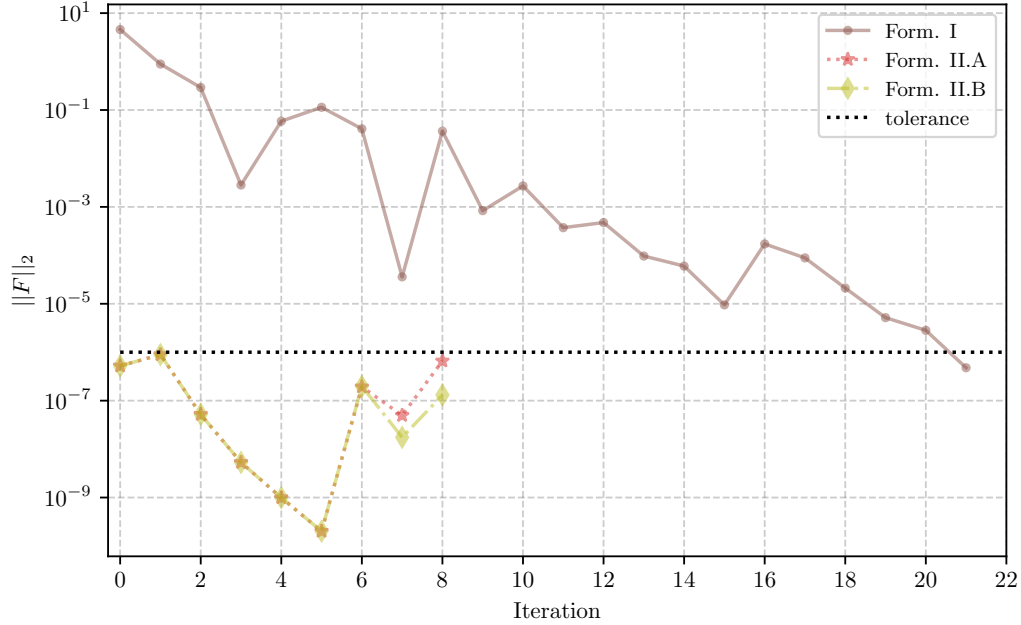
Figure 3: Error of scaled LF equations $||\boldsymbol{F}||_2$ at every iteration of the optimizer for network 1 (Figure 2a), for the OF problem with soft bounds on $\boldsymbol{y}$, using SLSQP

than formulation II. Comparing the final error of the LF equations for formulation I an II for each case, given in the final column of both tables, we see that the errors are slightly different, meaning that the optimal solution found by formulation I and and formulation II are slightly different. Formulations II.A. and II.B show very similar performance. Hence, formulation II is more efficient than formulation I.

We find that there is no difference between soft and hard constraints. Based on this MES, trust-constrs performs worse than SLSQP and IPOPT. If bounds should be imposed on $\boldsymbol{u}$ or on $\boldsymbol{y}$ depends on the network and the optimizer. Finally, both formulation I and II can be used for the OF problem, and formulation II is more efficient than formulation I.

5.3 MES 2: Effect of LF formulations

The second MES consists of a base network, coupling 3-node single-carrier gas, electricity, and heat networks. For each carrier, node 1 is a source, and node 3 is a sink. For the electrical network and the heat network, node 2 is an additional source. We choose to couple these single-carrier networks at node 1 with a single EH, see Figure 4a. This base case can be extended by replacing the sink at node 3 of each single-carrier network by a tree-like structure which we call 'streets'. There are s streets, $S_1 - S_s$, which are all connected to node 3 of the base single-carrier network through a junction node. The streets consists of n loads, $L_1 - L_n$, connected to the main street links by junctions, m of which, $J_1 - J_m$, are connected to two loads. Figure 4b shows the topology of such an extended single-carrier network, consisting of $3 + s\,(2n - m + 1)$ nodes and $2 + s\,(2n - m + 1)$ links. The extended MES is created by coupling the single-carrier networks in the same way as for

the base network. See [27] for further details and the specific LF equations used.

(a) Coupled at node 1 with an EH.

(b) Extension of single-carrier networks.
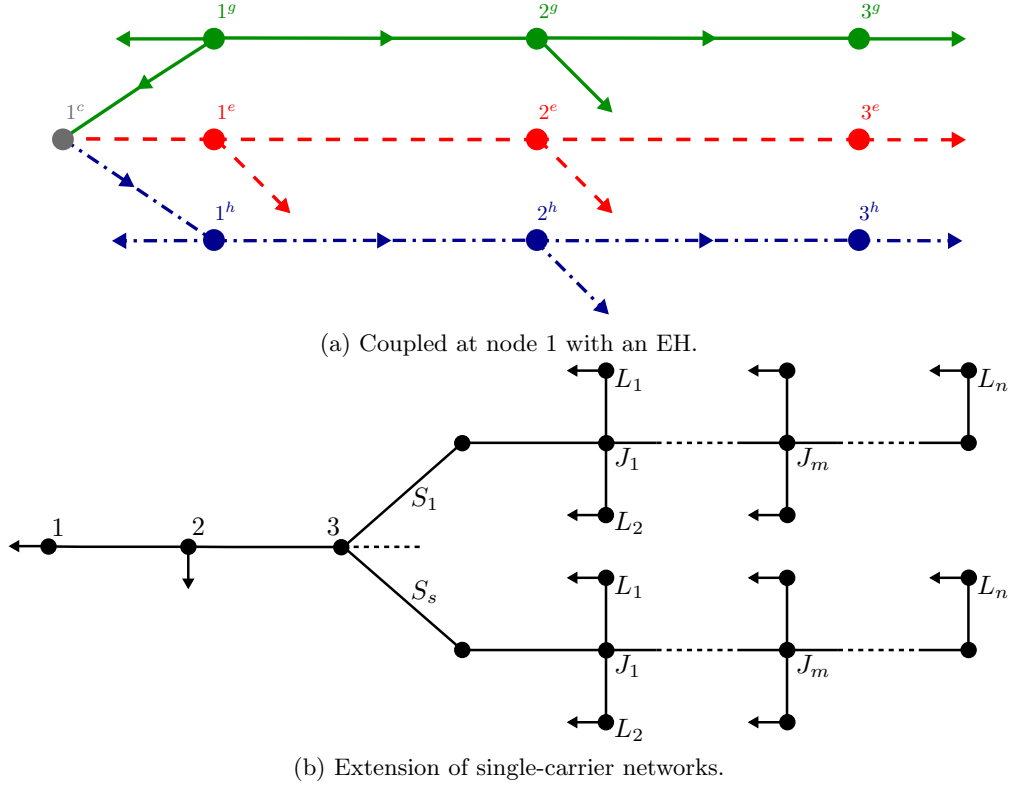
Figure 4: MES network topology, see also [27]. The multi-carrier base network (a) can be extended as (b). Arrows on links and terminal links show defined direction of flow.

We consider the base network, which is the network shown in Figure 4a, and an extended network with 163 nodes per single-carrier network ($n = 10, m = 5, s = 10$).

5.3.1   Problem Formulations

Nodes 1^g, 1^e, 2^e, and 2^h are external single-carrier sources. The EH produces electrical and heat power, such that is a source to the electrical and heat networks. The energy vector $\boldsymbol{E}$ in the objective function (3) is then

$$\boldsymbol{E} = \left(-\text{GHV}q_{1,0}, \; -P_{1,0}, \; -P_{2,0}, \; P_{1^c1^e}, \; -\Delta\varphi_{2,0}, \; \Delta\varphi_{1^c1^h}\right)^T \tag{17}$$

where $q_{1,0}$, $P_{1,0}$, $P_{2,0}$, $\Delta\varphi_{2,0} < 0$ and $P_{1^c1^e}$, $\Delta\varphi_{1^c1^h} > 0$.

Table 5 gives the BCs of the base network used in the LF problem. For the extended networks, the additional nodes are load or junction nodes. We take some of these known variables as control variables in OF:

$$\boldsymbol{u} = \left(|V_2|, \; P_2, \; T_{2,0}^s, \; \Delta\varphi_{2,0}\right)^T \tag{18}$$

21

Table 5: Boundary conditions for steady-state LF for the network in Figure 4.

Node	Type	Specified	Unknown
1^g	ref.	p^g	q
2^g	load	$q = 0$	p^g
3^g	load	q	p^g
1^e	QVδ	Q, $|V|$, δ	P
2^e	gen.	P, $|V|$	Q, δ
3^e	load	P, Q	$|V|$, δ
1^h	junction ref. temp.	T^s, p^h, $m = 0$	T^r
2^h	load (source)	$T^s_{2,0}$, $\Delta\varphi_{2,0} < 0$	T^s, T^r, p^h, $m_{2,0}$
3^h	load (sink)	$T^r_{3,0}$, $\Delta\varphi_{3,0} > 0$	T^s, T^r, p^h, $m_{3,0}$
1^c	standard	-	$T^s_{1^c 1^h}$

We use two formulations of the LF equations in the gas part, and two in the heat part. In a gas network, the general steady-state flow equation of a pipe [10], represented by a link k from node i to node j, can either express the link flow as a function of pressures, denoted as $f^{q(\Delta p)}$, or express the pressure drop as a function of link flow, denoted by $f^{\Delta p(q)}$. Defining the pressure drop by $\Delta p^g_k := (p^g_i)^2 - (p^g_j)^2$, we have

$$f_k^{q(\Delta p)} := q_k - C^g_k \text{sign}\left(\Delta p^g_k\right) \left(f^g_k\right)^{-\frac{1}{2}} |\Delta p^g_k|^{\frac{1}{2}} = 0 \tag{19a}$$

$$f_k^{\Delta p(q)} := \Delta p^g_k - \left(C^g_k\right)^{-2} f^g_k |q_k| q_k = 0 \tag{19b}$$

with q_k the link flow, p^g_i the nodal pressure, f^g_k the friction factor, and C^g_k the pipe constant. We use the nodal or the full formulation to collect the LF equations into a system of equations for the gas part. In the nodal formulation, the link equations (19a) are substituted in nodal conservation of mass. In the full formulation, the link equations are not substituted. We use link equations (19b) for the full formulation. In the nodal formulation, the link flows q_k are derived variables, while they are part of the state variables $\boldsymbol{x}$ in the full formulation.

For the heat load nodes i we assume that the outflow temperature directly after the heat exchanger, modeled by a terminal link l, is known. That is, the terminal link supply temperature $T^s_{i,l}$ is known for sources, and the terminal link return temperature $T^r_{i,l}$ is known for sinks. We use the standard or the terminal link formulation to collect the LF equations into a hydraulic-thermal system of equations for the heat part [27]. In the terminal link formulation, the terminal link flows $m_{i,l}$ are part of the state variables $\boldsymbol{x}$, and nodal conservation of mass is a linear equation. In the standard formulation, the heat power equation is used to eliminate the terminal link mass flows, reducing the system size of the LF problem. Nodal conservation of mass becomes nonlinear, and the flows $m_{i,l}$ are derived variables.

If the link gas flows q_k or terminal link mass flow $m_{i,l}$ are derived variables, we do not include

them in $\boldsymbol{x^G}$. The extended state variables are then:

$$\boldsymbol{x^{G,g}} = \left(q_{1,0}\right) \tag{20a}$$

$$\boldsymbol{x^{G,e}} = \left(P_{1,0},\ Q_{2,0}\right) \tag{20b}$$

$$\boldsymbol{x_n^{F,g}} = \left(p_2^g,\ p_3^g\right)^T \tag{20c}$$

$$\boldsymbol{x_f^{F,g}} = \left(q_{12},\ q_{32},\ p_2^g,\ p_3^g\right)^T \tag{20d}$$

$$\boldsymbol{x^{F,e}} = \left(\delta_2,\ \delta_3,\ |V_3|\right)^T \tag{20e}$$

$$\boldsymbol{x_s^{F,h}} = \left(m_{12},\ m_{23},\ p_2^h,\ p_3^h,\ T_2^s,\ T_3^s\,T_1^r,\ T_2^r,\ T_3^r\right)^T \tag{20f}$$

$$\boldsymbol{x_t^{F,h}} = \left(m_{12},\ m_{23},\ m_{2,0},\ m_{3,0},\ p_2^h,\ p_3^h,\ T_2^s,\ T_3^s\,T_1^r,\ T_2^r,\ T_3^r\right)^T \tag{20g}$$

$$\boldsymbol{x^{F,c}} = \left(q_{1^g1^c},\ P_{1^c1^e},\ Q_{1^c1^e},\ m_{1^c1^h},\ \Delta\varphi_{1^c1^h},\ T_{1^c1^h}^s\right)^T \tag{20h}$$

with $\boldsymbol{x_n^{F,g}}$ and $\boldsymbol{x_f^{F,g}}$ the gas state variables using the nodal or the full formulation, and $\boldsymbol{x_s^{F,h}}$ and $\boldsymbol{x_t^{F,h}}$ the heat state variables using the standard or terminal link formulation.

The extended LF problem (4) is not solvable (for a physically feasible solution) for all values of $\boldsymbol{u}$. The bounds imposed on $\boldsymbol{u}$ are chosen such that the LF problem is solvable. We also impose bounds on the (extended) state variables $\boldsymbol{x^{G,g}}$, $\boldsymbol{x^{G,e}}$, $\boldsymbol{x^{F,g}}$, $\boldsymbol{x^{F,e}}$, $\boldsymbol{x^{F,h}}$, and $\boldsymbol{x^{F,c}}$. In addition, we consider imposing bounds on the gas link mass flows q_k, electrical link complex power $|S_k|^2 = P_k^2 + Q_k^2$, and heat terminal mass flows $m_{i,l}$. For the nodal and standard formulation, q_k and $m_{i,l}$ are derived variables, as is $|S_k|^2$. Bounds are imposed by (nonlinear) inequality constraints (5c) or (6c). For each gas and electrical link k and each heat terminal link l, the inequality constraints are:

$$\boldsymbol{\gamma_k^g} = \begin{pmatrix} q_k(p_i,\ p_j) - q_k^{lb} \\ q_k^{ub} - q_k(p_i,\ p_j) \end{pmatrix} \tag{21a}$$

$$\gamma_k^e = (|S_k|^2)^{ub} - P_k^2 - Q_k^2 \tag{21b}$$

$$\boldsymbol{\gamma_{i,l}^h} = \begin{pmatrix} m_{i,l}\left(\Delta\varphi_{i,l},\ T_{i,l}^s,\ T_{i,l}^r\right) - m_{i,l}^{lb} \\ m_{i,l}^{ub} - m_{i,l}\left(\Delta\varphi_{i,l},\ T_{i,l}^s,\ T_{i,l}^r\right) \end{pmatrix} \tag{21c}$$

Here, the heat terminal link mass flow $m_{i,l}$ is a function of terminal link heat powers $\Delta\varphi_{i,l}$, terminal link supply temperature $T_{i,l}^s$, and terminal link return temperature $T_{i,l}^r$ using the heat power equation.

If the full formulation is used in gas, and the terminal link formulation is used in heat, q_k and $m_{i,l}$ are part of $\boldsymbol{x^F}$. If bounds are then imposed on these variables, they are included as bounds (5e) or (6d) instead of using (21a) and (21c).

We have seen in Section 5.2 that there is no difference between using soft or hard constraints in the optimizers, so we only consider soft constraints for this network. Furthermore, we do not consider the trust-constr optimizer, since it performs worse than SLSQP and IPOPT.

This gives a total of 24 formulations and solution methods of the OF problems. That is, we use formulation I (5) for the OF problem, including the LF equations as equality constraints, or we use formulation II (6), eliminating LF equations. For the latter, we can use the direct approach II.A or the adjoint approach II.B when solving the optimization problem. For each of these, we use one of the four possible formulation of the LF problems, based on the nodal formulation with pipe flow equations (19a) or the full formulation with pipe flow equations (19b) in the gas part,

23

and the standard formulation or the terminal link formulation in the heat part. Moreover, we impose bounds on the (derived) variables q_k, $|S_k|^2$, and $m_{i,l}$, or we do not impose these bounds. In addition to these 24 options, we use matrix scaling or per unit scaling to scale the problem, and we use SLSQP and IPOPT as optimizers. Finally, we consider various sizes of the network.

Table 6 gives the system size of the OF problem for these 24 formulations, for the base network. The number of bounds on $x \in \boldsymbol{x}$ should be counted double, as they are lower and upper bounds. The system sizes are different for the various formulations. However, using the adjoint approach, or formulation II.B, always requires more linear systems to be solved than using the direct approach, or formulation II.A. For both approaches, the size of the linear systems is equal, since $\boldsymbol{h_x}$ is square.

Table 6: Size of $\boldsymbol{u}$, $\boldsymbol{x^G}$, $\boldsymbol{x^F}$, $\boldsymbol{\gamma}$, and the number of $x \in \boldsymbol{x}$ on which bounds are imposed, for the various formulations of the OF problem for the base network. The last two columns give the number and size of the linear systems (10c) and (11c)–(11d) for formulation II.A en II.B.

bounds on q_k, $|S_k|^2$, $m_{i,l}$	form. gas	form. heat	$\boldsymbol{x^G}$	$\boldsymbol{x^F}$	$\boldsymbol{u}$	$\boldsymbol{\gamma}$	#x with bounds	OF form.	# lin. sys.	size lin. sys.
no	full	term. link	3	24	4	0	23	II.A	4	27×27
								II.B	47	27×27
		standard	3	22	4	0	23	II.A	4	25×25
								II.B	47	25×25
	nodal	term. link	3	22	4	0	23	II.A	4	25×25
								II.B	47	25×25
		standard	3	20	4	0	23	II.A	4	23×23
								II.B	47	23×23
yes	full	term. link	3	24	4	2	27	II.A	4	27×27
								II.B	57	27×27
		standard	3	22	4	6	25	II.A	4	25×25
								II.B	57	25×25
	nodal	term. link	3	22	4	6	25	II.A	4	25×25
								II.B	57	25×25
		standard	3	20	4	10	23	II.A	4	23×23
								II.B	57	23×23

5.3.2 Results

We set the tolerance for the OF problem, for the extended LF problem ε, and τ to 10^{-6}. The maximum number of iterations for the optimizers is 50, and 10 for Newton's method to solve the extended LF problem (4) within formulation II. We have found that the optimizers were unlikely to find a solution if it did not find one within these 50 iterations.

Figures 5 and 6 show the difference in the energy flows of the sources between a reference LF solution and optimal solutions. For the gas input, only the part of the total gas input into node 1 that is used by the coupling is shown, that is, only $-q_1 - q_3$ is shown. We can see that energy flows of the optimal solution are distributed differently over the sources compared with the LF

solution. Most significantly, $P_1 \approx 0$ for the optimal solutions. However, Figure 5b shows that the total active power and heat power of the sources are roughly equal. Since $P_1 \approx 0$, the total gas input $-q_1$ is bigger for the optimal solutions, as we can see in Figure 5a. Figure 6 shows that the total generation costs of the optimal solutions are lower than those of the reference LF solution, as expected.

Tables 7 and 8 give the results for the base network, using matrix scaling and per unit scaling respectively. Again, a '-' indicates the optimizer did not find a solution for that particular case.

Table 7: Information on optimizers of the optimal flow problem for the base network, using matrix scaling.

bounds on q_k, $\lvert S_k\rvert^2$, $m_{i,l}$	form. gas	form. heat	OF form.	# iters		# f		$\lvert\lvert\boldsymbol{F}\rvert\rvert_2$	
				SLSQP	IPOPT	SLSQP	IPOPT	SLSQP	IPOPT
no	full	term. link	I	14	41	24	59	$3.011 \cdot 10^{-14}$	$4.320 \cdot 10^{-11}$
			II.A	15	-	46	-	$6.920 \cdot 10^{-11}$	-
			II.B	15	-	46	-	$6.917 \cdot 10^{-11}$	-
		standard	I	17	13	25	14	$3.874 \cdot 10^{-13}$	$1.991 \cdot 10^{-9}$
			II.A	6	-	16	-	$6.078 \cdot 10^{-11}$	-
			II.B	6	-	16	-	$6.087 \cdot 10^{-11}$	-
	nodal	term. link	I	13	16	23	18	$6.025 \cdot 10^{-12}$	$3.063 \cdot 10^{-8}$
			II.A	-	-	-	-	-	-
			II.B	49	-	50	-	$9.439 \cdot 10^{-11}$	-
		standard	I	14	19	17	20	$5.250 \cdot 10^{-14}$	$2.140 \cdot 10^{-7}$
			II.A	7	10	7	11	$2.791 \cdot 10^{-12}$	$6.706 \cdot 10^{-9}$
			II.B	7	10	7	11	$2.851 \cdot 10^{-12}$	$6.706 \cdot 10^{-9}$
yes	full	term. link	I	12	27	22	33	$6.589 \cdot 10^{-12}$	$1.306 \cdot 10^{-9}$
			II.A	7	21	7	29	$2.850 \cdot 10^{-12}$	$1.077 \cdot 10^{-9}$
			II.B	7	21	7	29	$2.791 \cdot 10^{-12}$	$1.077 \cdot 10^{-9}$
		standard	I	16	36	32	42	$1.969 \cdot 10^{-11}$	$2.311 \cdot 10^{-13}$
			II.A	7	48	7	117	$2.761 \cdot 10^{-12}$	$8.024 \cdot 10^{-7}$
			II.B	7	-	7	-	$2.791 \cdot 10^{-12}$	-
	nodal	term. link	I	11	29	12	35	$1.145 \cdot 10^{-9}$	$2.827 \cdot 10^{-9}$
			II.A	7	21	7	29	$2.821 \cdot 10^{-12}$	$1.077 \cdot 10^{-9}$
			II.B	7	21	7	29	$2.851 \cdot 10^{-12}$	$1.077 \cdot 10^{-9}$
		standard	I	14	40	17	97	$1.686 \cdot 10^{-14}$	$6.655 \cdot 10^{-14}$
			II.A	7	18	7	26	$2.791 \cdot 10^{-12}$	$2.197 \cdot 10^{-12}$
			II.B	7	18	7	26	$2.732 \cdot 10^{-12}$	$2.197 \cdot 10^{-12}$

For the base case, SLSQP is able to find a solution for slightly more options of the OF problem than IPOPT. When both find a solution, SLSPQ converges significantly faster than IPOPT.

Then, we consider the effect of imposing bounds on q_k, $m_{i,l}$ en $\lvert S_k\rvert^2$. If bounds are imposed, an optimal solution is found for more options of the OF problem, both in Table 7 and Table 8. The number of iterations required to find a solution is roughly equal with or without these bounds, except for one case. With nodal formulation in gas and standard formulation in heat, IPOPT requires significantly more iterations if bounds are imposed than if they are not imposed, for all three formulations I, II.A, and II.B.

Comparing the various formulations of the LF equations in Tables 7 and 8, that is, nodal or

Table 8: Information on optimizers of the optimal flow problem for base network, using per unit scaling.

bounds on q_k, $|S_k|^2$, $m_{i,l}$	form. gas	form. heat	OF form.	# iters		# f		$||\boldsymbol{F}||_2$	
				SLSQP	IPOPT	SLSQP	IPOPT	SLSQP	IPOPT
no	full	term. link	I	12	41	22	59	$6.601 \cdot 10^{-12}$	$4.316 \cdot 10^{-11}$
			II.A	15	-	46	-	$6.911 \cdot 10^{-11}$	-
			II.B	15	-	46	-	$6.920 \cdot 10^{-11}$	-
		standard	I	16	13	32	14	$1.900 \cdot 10^{-11}$	$1.991 \cdot 10^{-9}$
			II.A	6	-	16	-	$6.076 \cdot 10^{-11}$	-
			II.B	6	-	16	-	$6.080 \cdot 10^{-11}$	-
	nodal	term. link	I	13	16	23	18	$6.049 \cdot 10^{-12}$	$3.063 \cdot 10^{-8}$
			II.A	-	-	-	-	-	-
			II.B	-	-	-	-	-	-
		standard	I	16	19	31	20	$3.224 \cdot 10^{-14}$	$2.140 \cdot 10^{-7}$
			II.A	7	10	7	11	$2.863 \cdot 10^{-12}$	$6.706 \cdot 10^{-9}$
			II.B	7	10	7	11	$2.862 \cdot 10^{-12}$	$6.706 \cdot 10^{-9}$
yes	full	term. link	I	12	27	13	33	$1.532 \cdot 10^{-12}$	$1.306 \cdot 10^{-9}$
			II.A	7	21	7	29	$2.749 \cdot 10^{-12}$	$1.077 \cdot 10^{-9}$
			II.B	7	21	7	29	$2.805 \cdot 10^{-12}$	$1.077 \cdot 10^{-9}$
		standard	I	16	36	32	42	$1.926 \cdot 10^{-11}$	$2.418 \cdot 10^{-13}$
			II.A	7	20	7	28	$2.750 \cdot 10^{-12}$	$1.651 \cdot 10^{-10}$
			II.B	7	20	7	28	$2.805 \cdot 10^{-12}$	$1.651 \cdot 10^{-10}$
	nodal	term. link	I	13	29	23	35	$6.037 \cdot 10^{-12}$	$2.827 \cdot 10^{-9}$
			II.A	7	21	7	29	$2.805 \cdot 10^{-12}$	$1.077 \cdot 10^{-9}$
			II.B	7	21	7	29	$2.806 \cdot 10^{-12}$	$1.077 \cdot 10^{-9}$
		standard	I	14	33	17	91	$5.623 \cdot 10^{-14}$	$3.007 \cdot 10^{-11}$
			II.A	7	18	7	26	$2.777 \cdot 10^{-12}$	$2.198 \cdot 10^{-12}$
			II.B	7	18	7	26	$2.805 \cdot 10^{-12}$	$2.198 \cdot 10^{-12}$

full formulation in gas and standard or terminal link formulation in heat, we can see that the number of iterations required to find a solution are not the same for the various formulations. These differences are minor, expect for one case. For the OF problem without bounds on q_k, $m_{i,l}$, and $|S_k|^2$, nodal formulation in gas, and terminal link flow formulation in heat, a solution is not found with formulation II. This shows that the formulation of the system of LF equations influences the solvability of the OF problem and influences the convergence of the optimizers.

We compare Table 7 with Table 8 to look at the effect of scaling. There are minor differences between matrix scaling and per unit scaling. With matrix scaling (Table 7), SLSQP with II.B finds a solution for the OF problem without bounds on q_k, $m_{i,l}$, and $|S_k|^2$, nodal formulation in gas, and terminal link formulation in heat, while no solution is found with per unit scaling (Table 8). On the other hand, with per unit scaling, IPOPT with II.B finds a solution for the OF problem with bounds on q_k, $m_{i,l}$, and $|S_k|^2$, full formulation in gas, and standard formulation in heat, while no solution is found with matrix scaling. Furthermore, there is some difference in the number of iterations when a solution is found with both types of scaling. Compare, for instance, SLSQP with I for the OF problem without bounds on q_k, $m_{i,l}$, and $|S_k|^2$, full formulation in gas, and terminal link flow formulation in heat, or SLSQP with I for the OF problem with bounds on q_k, $m_{i,l}$, and

$|S_k|^2$, nodal formulation in gas, and terminal link flow formulation in heat. Finally, the solutions found with matrix scaling are slightly different from the ones found with per unit scaling, even if the number of iterations of the optimizers are the same. Compare, for instance, the LF error in Table 7 with Table 8, for SLSQP for the OF problem with bounds on q_k, $m_{i,l}$, and $|S_k|^2$, full formulation in gas, and terminal link flow formulation in heat.

The difference between matrix and per unit scaling is illustrated in Figure 7, which shows the error of LF equations $||\boldsymbol{F}||_2$ at each iteration of the optimizer for the base network. The results are shown for the OF problem without bounds on q_k, $m_{i,l}$, and $|S_k|^2$, nodal formulation in gas, and terminal link flow formulation in heat, using SLSQP and formulation I. The figure shows that the iterates give different values of the scaled LF equations, indicating that matrix scaling and per unit scaling result in different iterates, even if the same base values are used. We have seen similar results for MES 1 and for the extended network of MES 2. Therefore, matrix scaling and per unit scaling are not equivalent if solving the OF problem.

Finally, we consider the inclusion of the LF equations in the OF problem, that is, we compare formulation I with formulation II. For this network, there are some options of the OF problem where a solution is found using formulation I but not when using formulation II.A or II.B. However, if all three formulation I, II.A, and II.B find a solution, formulation II requires significantly fewer iterations than formulation I.

Table 9 gives the results for the network with 163 nodes per single-carrier network, using matrix scaling.

For this extended network, SLSQP and IPOPT find a solution in the same cases, although IPOPT requires more iterations than SLSQP.

As for the base network, we see in Table 9 that the formulation of the LF problem influences the solvability of the OF problem and influences the convergence of the optimizers. Most notably, no solution is found for the OF problem with bounds on q_k, $m_{i,l}$, and $|S_k|^2$, full formulation in gas, and standard formulation in heat. SLSQP requires more iterations for the the OF problem with bounds on q_k, $m_{i,l}$, and $|S_k|^2$, nodal formulation in gas, and standard formulation in heat, than for the other cases. IPOPT requires fewer iterations for the the OF problem without bounds on q_k, $m_{i,l}$, and $|S_k|^2$ and nodal formulation in gas, than for the other OF formulations.

Finally, we compare formulations I, II.A, and II.B. No solution is found using formulation I, for any of the formulations of LF. Furthermore, there are some differences between formulation II.A and II.B, both for SLSQP and IPOPT. The difference is biggest for the OF problem without bounds on q_k, $m_{i,l}$, and $|S_k|^2$, nodal formulation in gas, and standard formulation in heat, using SLSQP. This is illustrated in Figure 8, which shows the error of LF equations $||\boldsymbol{F}||_2$ at each iteration of the optimizer for this case. We can see that formulations II.A and II.B result in different iterates and a different number of iterates. For the other cases there are minor differences. Therefore, formulations II.A and II.B are not equivalent.

Based on this MES, we find that matrix scaling and per unit scaling are not equivalent when solving the OF problem. Neither are formulations II.A and II.B. The formulation of the LF equations influences the solvability of the OF problem, and the convergence of the optimizers. If a solution is found for all three formulations I, II.A, and II.B, formulation II requires significantly fewer iterations than formulation I.

Table 9: Information on optimizers of the optimal flow problem for the extended network (163 nodes per carrier, $n = 10, m = 5, s = 10$), using matrix scaling.

bounds on q_k, $|S_k|^2$, $m_{i,l}$	form. gas	form. heat	OF form.	# iters		# f		$||\boldsymbol{F}||_2$	
				SLSQP	IPOPT	SLSQP	IPOPT	SLSQP	IPOPT
no	full	term. link	I	-	-	-	-	-	-
			II.A	5	24	5	40	$1.307 \cdot 10^{-12}$	$5.825 \cdot 10^{-7}$
			II.B	5	24	5	40	$1.578 \cdot 10^{-12}$	$5.825 \cdot 10^{-7}$
		standard	I	-	-	-	-	-	-
			II.A	3	24	3	40	$2.933 \cdot 10^{-10}$	$5.834 \cdot 10^{-7}$
			II.B	3	24	3	40	$2.933 \cdot 10^{-10}$	$5.834 \cdot 10^{-7}$
	nodal	term. link	I	-	-	-	-	-	-
			II.A	5	15	5	40	$1.368 \cdot 10^{-12}$	$1.532 \cdot 10^{-12}$
			II.B	5	15	5	40	$1.399 \cdot 10^{-12}$	$1.148 \cdot 10^{-12}$
		standard	I	-	-	-	-	-	-
			II.A	15	14	15	22	$2.318 \cdot 10^{-11}$	$1.678 \cdot 10^{-12}$
			II.B	3	14	3	22	$2.933 \cdot 10^{-10}$	$2.152 \cdot 10^{-12}$
yes	full	term. link	I	-	-	-	-	-	-
			II.A	5	31	5	32	$1.309 \cdot 10^{-12}$	$1.903 \cdot 10^{-12}$
			II.B	5	32	5	33	$1.451 \cdot 10^{-12}$	$1.515 \cdot 10^{-12}$
		standard	I	-	-	-	-	-	-
			II.A	-	-	-	-	-	-
			II.B	-	-	-	-	-	-
	nodal	term. link	I	-	-	-	-	-	-
			II.A	5	30	5	31	$1.368 \cdot 10^{-12}$	$4.251 \cdot 10^{-7}$
			II.B	5	28	5	29	$1.399 \cdot 10^{-12}$	$4.520 \cdot 10^{-10}$
		standard	I	-	-	-	-	-	-
			II.A	12	28	14	30	$5.331 \cdot 10^{-11}$	$6.984 \cdot 10^{-7}$
			II.B	12	28	13	30	$1.608 \cdot 10^{-10}$	$6.985 \cdot 10^{-7}$
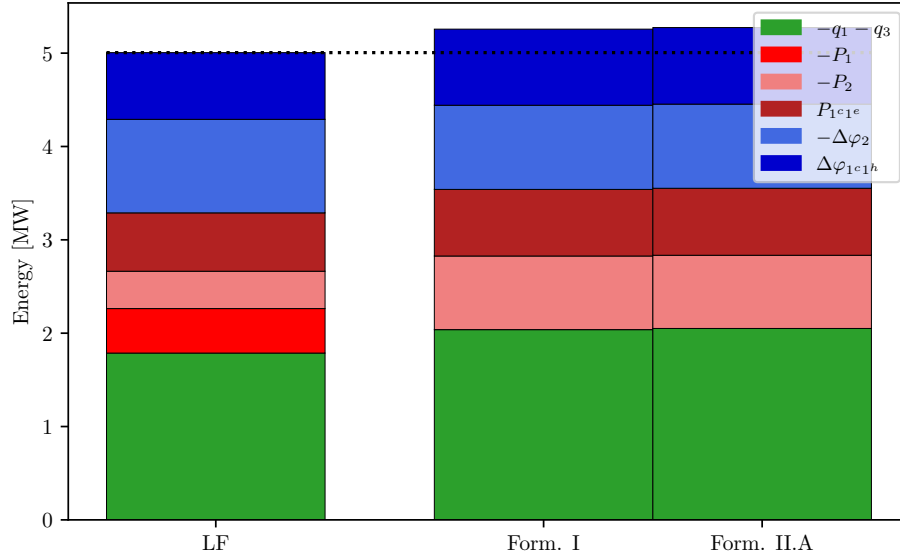
(a) With gas input; the part that goes towards the coupling.
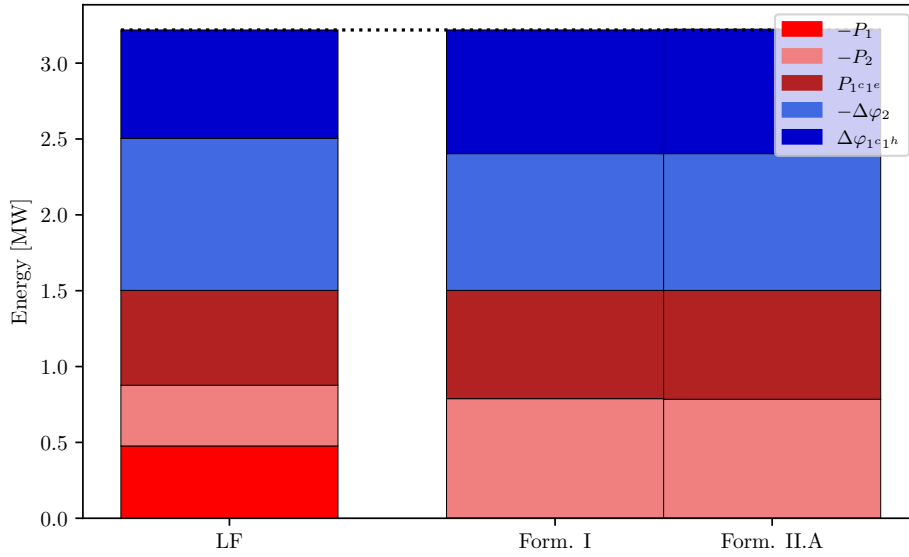
(b) Without gas input

Figure 5: Energy of sources $\boldsymbol{E}$ for the base network. The first bar shows a reference LF solution, the others OF solutions, without bounds on q_k, $m_{i,l}$, and $|S_k|^2$, full formulation in gas, terminal link flow formulation in heat, using SLSQP and matrix scaling.
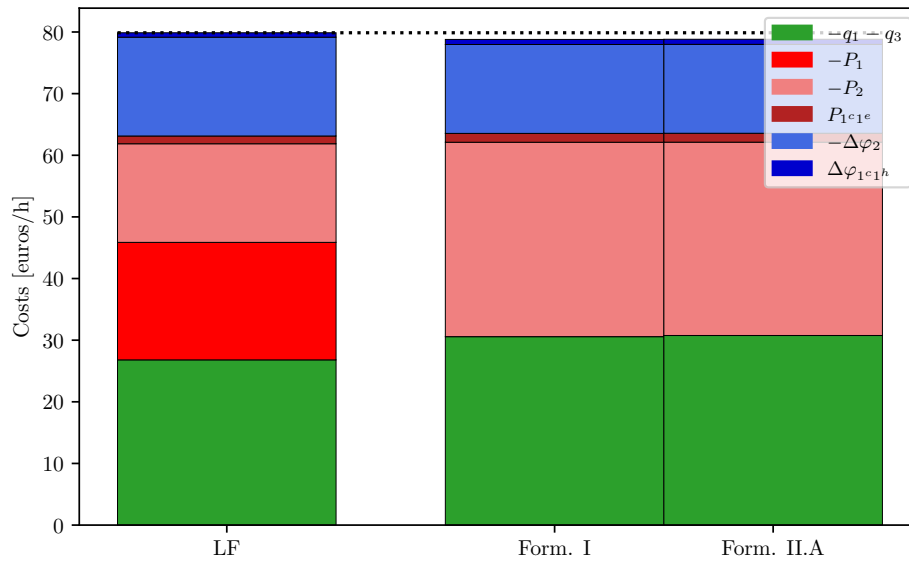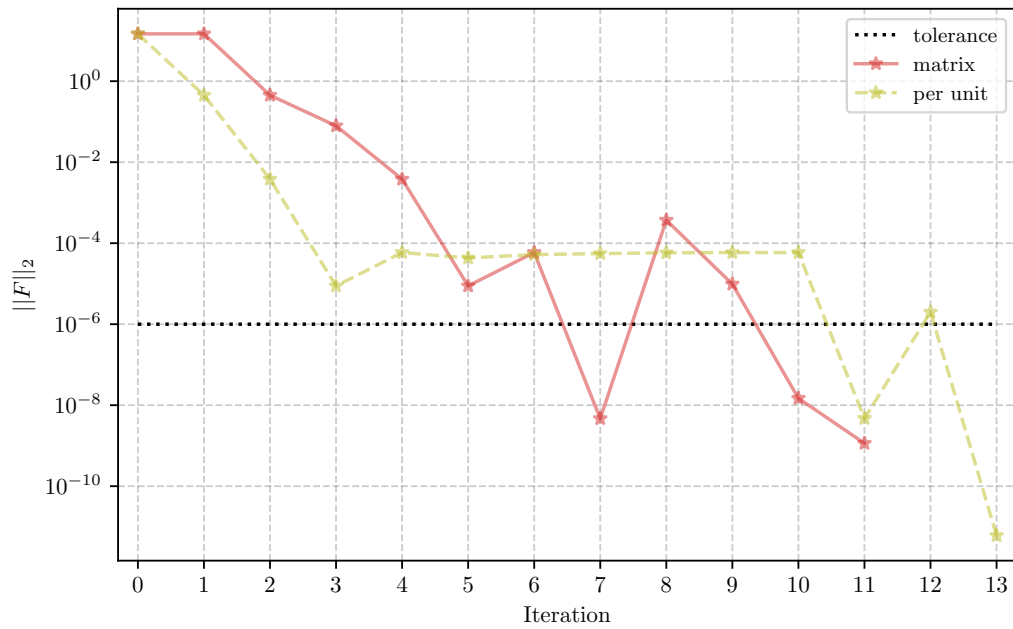
Figure 6: Generation costs for the base network. The gas input is only the part that goes towards coupling. The first bar shows a reference LF solution, the others OF solutions, without bounds on q_k, $m_{i,l}$, and $|S_k|^2$, full formulation in gas, terminal link flow formulation in heat, using SLSQP and matrix scaling.

Figure 7: Error of scaled LF equations $||\boldsymbol{F}||_2$ at every iteration of the optimizer for the OF problem of the base network, without bounds on q_k, $m_{i,l}$, and $|S_k|^2$, nodal formulation in gas, and terminal link flow formulation in heat, using formulation I and SLSQP. Comparison of matrix scaling and per unit scaling.
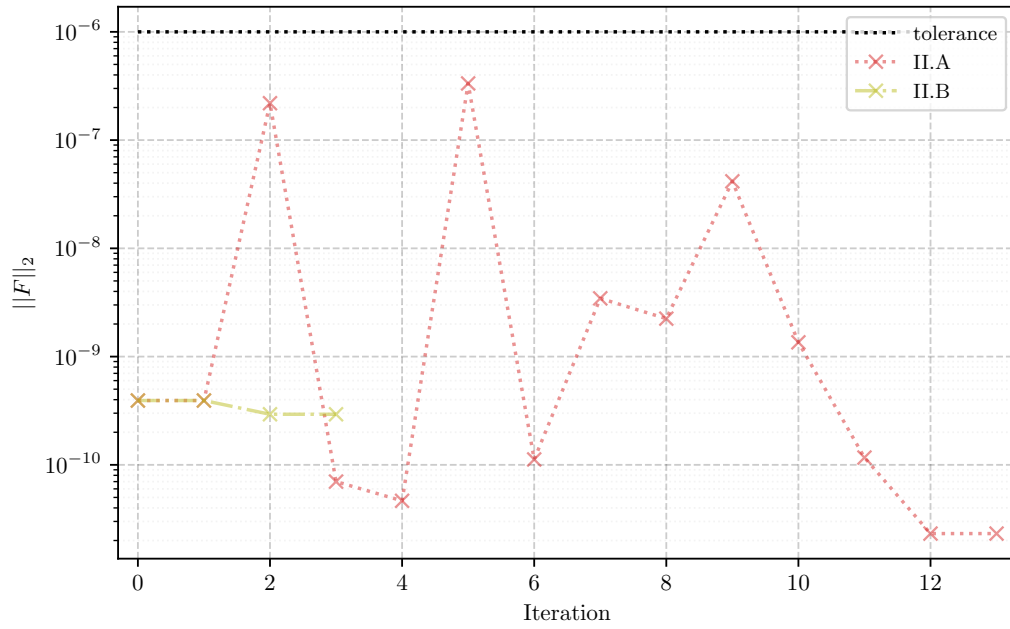
Figure 8: Error of scaled LF equations $||\boldsymbol{F}||_2$ at every iteration of the optimizer for the extended network (163 nodes per carrier, $n = 10, m = 5, s = 10$), bounds on q_k, $m_{i,l}$, and $|S_k|^2$, nodal formulation in gas, and standard formulation in heat, using SLSQP. Comparison of formulation II.A. and formulation II.B.

6 Conclusion

We optimize the operation of multi-carrier energy systems (MESs) by minimizing total energy generation costs while satisfying the steady-state load flow equations (LF) and other physical network limits. We compare two ways of including the LF equations within the optimal flow (OF) problem: formulation I and formulation II. Formulation I includes the LF equations explicitly in OF, as equality constraints. Formulation II includes the LF equations as subsystem in OF, using nonlinear elimination of variables and equations. In addition to these two formulations, we consider the effect of scaling, formulation of the LF equations, and imposing bounds on the solvability of the OF problem. To solve the resulting OF problems and to consider converge, we use three optimizers, and two approaches with formulation II: the direct approach (II.A) or the adjoint approach (II.B).

Scaling is needed to solve the OF problem for MESs. Both matrix scaling and per unit scaling can be used. The are not equivalent for optimization, resulting in different iterates of the optimizers.

The formulation of the LF equations, both the individual equations and the system of equations, influences the solvability and convergence of the OF problem. The formulation of the system of LF equations determines which variables are state variables and which are derived variables, which subsequently determines the nonlinearity of the (in)equality constraints and objective function. The formulation of the system of LF equations is related to the choice of boundary conditions for the LF problem, which determines the choice of control variables in the OF problem. The best formulation of the LF equations, and the best choice for the control variables, depends on the specific problem and network.

Bounds on the control variables are used to keep the iterates (physically) feasible, by ensuring the extended LF problem is solvable. Hence, choosing appropriate bounds for the control variables is crucial in formulating a solvable OF problem. Additional bounds on (extended) state variables and derived variables increase the complexity of the optimization problem and (can) increase the nonlinearity. Hence, they influence the solvability of the OF problem and the convergence of the optimizers. Whether bounds should be imposed depends on the specific problem and energy system.

Including the LF equations as equality constraints or as subsystem both result in a solvable OF problem. That is, both formulation I and formulation II can be used to optimize a MES. Formulation II reduces the size of the optimization space compared with formulation I, but increases the nonlinearity of the objective function and constraints. In formulation II, the LF equations are solved separately for multiple iterations of the optimizer. This allows the use of a dedicated, separate, solver for the LF problem. Furthermore, it ensures the LF equations are satisfied at each iteration of the optimizer. However, it might increase CPU time.

For the two example MESs, formulation II requires significantly fewer iterations than formulation I, if an optimal solution is found for both formulations. Furthermore, formulations II.A and II.B are not equivalent. For some OF problems, II.A and II.B result in different iterates of the optimizers.

The OF problem for a MES can be formulated in various ways, with respect to choice of state variables, control variables, and boundary condition, with respect to the formulation of the LF equations, with respect to including the LF equations in the OF problem, with respect to scaling, and with respect to bounds and inequality constraints. Which way is best depends on the specific network and problem considered.

References

[1] Pierluigi Mancarella. MES (multi-energy systems): An overview of concepts and evaluation models. *Energy*, 65:1–17, jul 2014.

[2] Seungwon An, Qing Li, and T.W. Gedra. Natural gas and electricity optimal power flow. *IEEE PES Transmission and Distribution Conference and Exposition*, pages 138–143, 2003.

[3] Martin Geidl and Göran Andersson. Optimal Power Flow of Multiple Energy Carriers. *IEEE Transactions on Power Systems*, 22(1):145–155, 2007.

[4] Amin Shabanpour-Haghighi and Ali Reza Seifi. Simultaneous integrated optimal energy flow of electricity, gas, and heat. *Energy Conversion and Management*, 101:579–591, 2015.

[5] P. N. Biskas, N. G. Kanelakis, A. Papamatthaiou, and I. Alexandridis. Coupled optimization of electricity and natural gas systems using augmented Lagrangian and an alternating minimization method. *International Journal of Electrical Power & Energy Systems*, 80:202–218, 2016.

[6] Emmanouil Loukarakis and Pierluigi Mancarella. A sequential programming method for multi-energy districts optimal power flow. *2017 IEEE Manchester PowerTech, Powertech 2017*, pages 1–6, 2017.

[7] Zhengmao Li and Yan Xu. Optimal coordinated energy dispatch of a multi-energy microgrid in grid-connected and islanded modes. *Applied Energy*, 210:974–986, 2018.

[8] Eduardo Alejandro Martínez Ceseña and Pierluigi Mancarella. Energy Systems Integration in Smart Districts: Robust Optimization of Multi-Energy Flows in Integrated Electricity, Heat and Gas Networks. *IEEE Transactions on Smart Grid*, 10(1):1122–1131, January 2019.

[9] Pieter Schavemaker and Lou Van der Sluis. *Electrical power system essentials*. Wiley, Chichester, West Sussex, 2008.

[10] Andrzej J. Osiadacz. *Simulation and analysis of gas networks*. Spon, London, 1987.

[11] Xuezhi Liu and Pierluigi Mancarella. Modelling, assessment and Sankey diagrams of integrated electricity-heat-gas networks in multi-vector district energy systems. *Applied Energy*, 167:336–352, 2016.

[12] Getnet Tadesse Ayele, Pierrick Haurant, Björn Laumert, and Bruno Lacarrière. An extended energy hub approach for load flow analysis of highly coupled district energy networks: Illustration with electricity and heating. *Applied Energy*, 212:850–867, December 2018.

[13] Anne S. Markensteijn, Johan E. Romate, and Cornelis Vuik. A graph-based model framework for steady-state load flow problems of general multi-carrier energy systems. *Applied Energy*, 280, December 2020.

[14] Baljinnyam Sereeter, Cornelis Vuik, and Cees Witteveen. On a comparison of Newton–Raphson solvers for power flow problems. *Journal of Computational and Applied Mathematics*, 360:157–169, 2019.

[15] Xuezhi Liu, Nick Jenkins, Jianzhong Wu, and Audrius Bagdanavicius. Combined analysis of electricity and heat networks. *Applied Energy*, 162:1238–1250, 2016.

[16] E. Gill, Philip, Walter Murray, and H. Wright, Margaret. *Practical Optimization*. Acadamic Press, London, 1981.

[17] Jorge Nodecal and Stephen J. Wright. *Numerical Optimization*. Springer, New York, second edition, 2006.

[18] Pauli Virtanen, Ralf Gommers, Travis E. Oliphant, Matt Haberland, Tyler Reddy, David Cournapeau, Evgeni Burovski, Pearu Peterson, Warren Weckesser, Jonathan Bright, Stéfan J. van der Walt, Matthew Brett, Joshua Wilson, K. Jarrod Millman, Nikolay Mayorov, Andrew R. J. Nelson, Eric Jones, Robert Kern, Eric Larson, C J Carey, İlhan Polat, Yu Feng, Eric W. Moore, Jake VanderPlas, Denis Laxalde, Josef Perktold, Robert Cimrman, Ian Henriksen, E. A. Quintero, Charles R. Harris, Anne M. Archibald, Antônio H. Ribeiro, Fabian Pedregosa, Paul van Mulbregt, and SciPy 1.0 Contributors. SciPy 1.0: Fundamental Algorithms for Scientific Computing in Python. *Nature Methods*, 17:261–272, 2020.

[19] Andreas Wächter and Lorenz T. Biegler. On the implementation of an interior-point filter line-search algorithm for large-scale nonlinear programming. *Math. Program.*, 106:25–57, 2006.

[20] Richard H. Byrd, Mary E. Hribar, and Jorge Nocedal. An interior point algorithm for large-scale nonlinear programming. *SIAM J. Optim.*, 9(4):877–900, 1999.

[21] Dieter Kraft. A software package for sequential quadratic programming. Technical Report DFVLR-FB 88-28, DLR German Aerospace Center – Institute for Flight Mechanics, Köln, Germany, 1998.

[22] John E. Jr. Dennis and Robert B. Schnabel. *Numerical Methods for Unconstrained Optimization and Nonlinear Equations*. Society for Industrial and Applied Mathematics, Philadelphia, PA, USA, 1996.

[23] Anne S. Markensteijn, Johan E. Romate, and Cornelis Vuik. Scaling of the steady-state load flow equations for multi-carrier energy systems. In *Numerical Mathematics and Advanced Applications ENUMATH 2019*, 2020.

[24] M. B. Giles and N. A. Pierce. An Introduction to the Adjoint Approach to Design. *Flow, Turbulence and Combustion*, 65:393–415, 2000.

[25] Linda Petzold, Shengtai Li, Yang Cao, and Radu Serban. Sensitivity analysis of differential-algebraic equations and partial differential equations. *Computers Chemical Engineering*, 30(10):1553 – 1559, 2006. Papers form Chemical Process Control VII.

[26] Amin Shabanpour-Haghighi and Ali Reza Seifi. An integrated steady-state operation assessment of electrical, natural gas, and district heating networks. *IEEE Transactions on Power Systems*, 31(5):3636–3647, 2016.

[27] Anne S. Markensteijn and Cornelis Vuik. Convergence of Newton's Method for Steady-State Load Flow Problems in Multi-Carrier Energy Systems. In *IEEE PES Innovative Smart Grid Technologies (ISGT Europe 2020)*, 2020.